

Journal Pre-proof

Design and synthesis of Imidazo[1,2-*b*]pyridazine IRAK4 inhibitors for the treatment of mutant MYD88 L265P diffuse large B-cell lymphoma

Yun Chen, Gang Bai, Yi Ning, Shi Cai, Tao Zhang, Peiran Song, Jinpei Zhou, Wenhui Duan, Jian Ding, Hua Xie, Huibin Zhang



PII: S0223-5234(20)30059-3

DOI: <https://doi.org/10.1016/j.ejmech.2020.112092>

Reference: EJMECH 112092

To appear in: *European Journal of Medicinal Chemistry*

Received Date: 30 November 2019

Revised Date: 21 January 2020

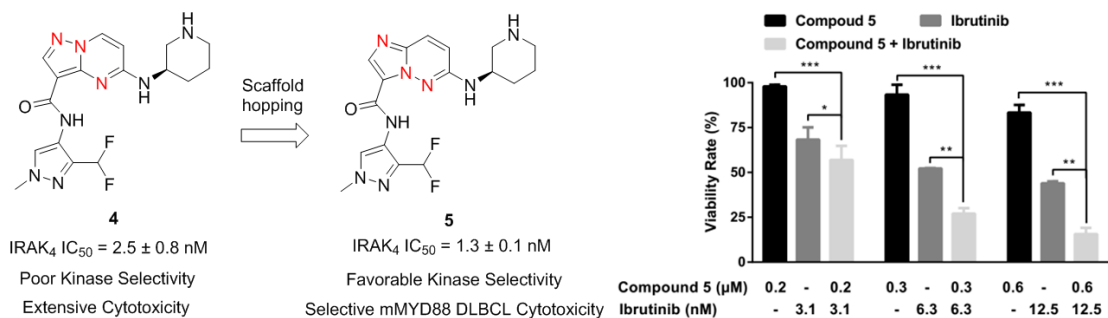
Accepted Date: 21 January 2020

Please cite this article as: Y. Chen, G. Bai, Y. Ning, S. Cai, T. Zhang, P. Song, J. Zhou, W. Duan, J. Ding, H. Xie, H. Zhang, Design and synthesis of Imidazo[1,2-*b*]pyridazine IRAK4 inhibitors for the treatment of mutant MYD88 L265P diffuse large B-cell lymphoma, *European Journal of Medicinal Chemistry* (2020), doi: <https://doi.org/10.1016/j.ejmech.2020.112092>.

This is a PDF file of an article that has undergone enhancements after acceptance, such as the addition of a cover page and metadata, and formatting for readability, but it is not yet the definitive version of record. This version will undergo additional copyediting, typesetting and review before it is published in its final form, but we are providing this version to give early visibility of the article. Please note that, during the production process, errors may be discovered which could affect the content, and all legal disclaimers that apply to the journal pertain.

© 2020 Published by Elsevier Masson SAS.

Graphical abstract



Journal Pre-proof

Design and Synthesis of Imidazo[1,2-*b*]pyridazine IRAK4 Inhibitors for the Treatment of Mutant MYD88 L265P Diffuse Large B-Cell Lymphoma

Yun Chen^{a,f,#}, Gang Bai^{b,c,d,#}, Yi Ning^{b,c}, Shi Cai^a, Tao Zhang^{b,c}, Peiran Song^{b,c}, Jinpei Zhou^e, Wenhui Duan^{c,f}, Jian Ding^{b,c,d}, Hua Xie^{b,c,*}, Huibin Zhang^{a,*}

^aCenter of Drug Discovery, State Key Laboratory of Natural Medicines, China Pharmaceutical University, 24 Tongjiaxiang, Nanjing 210009, PR China

^bState Key Laboratory of Drug Research, Shanghai Institute of Materia Medica, Chinese Academy of Sciences, Shanghai 201203, PR China

^cUniversity of Chinese Academy of Sciences, No. 19A Yuquan Road, Beijing 100049, China

^dSchool of Life Science and Technology, ShanghaiTech University, Shanghai 201210, PR China

^eDepartment of Medicinal Chemistry, China Pharmaceutical University, 24 Tongjiaxiang, Nanjing 210009, PR China

^fDepartment of Medicinal Chemistry, Shanghai Institute of Materia Medica, Chinese Academy of Sciences, 555 Zu Chong Zhi Road, Shanghai 201203, PR China

#Equal contribution: Both authors contributed equally to this work.

*Correspondence to: Huibin Zhang, E-mail : zhanghb80@163.com, Tel: 86-25-83271302;

Hua xie, E-mail : hxie@simm.ac.cn, Tel: 86-21-50805897.

Abstract

Harboring MYD88 L265P mutation triggers tumors growth through the activation of NF- κ B by interleukin-1 receptor associated kinase 4 (IRAK4) in diffuse large B-cell lymphoma (DLBCL), highlighting IRAK4 as a therapeutic target for tumors driven by aberrant MYD88 signaling. Herein, we report the design, synthesis, and structure–activity relationships of imidazo[1,2-*b*]pyridazines as potent IRAK4 inhibitors. The representative compound **5** exhibited excellent IRAK4 potency (IRAK4 IC₅₀ = 1.3 nM) and favorable kinase selectivity profile. It demonstrated cellular selectivity for activated B cell–like (ABC) subtype DLBCL with MYD88 L265P mutation in cytotoxicity assay. The kinase inhibitory efficiency of compound **5** was further validated by Western blot analysis of phosphorylation of IRAK4 and downstream signaling in OCI-LY10 and TMD8 cells. Besides, combination of compound **5** and BTK inhibitor ibrutinib synergistically reduced the viability of

TMD8 cells. These results indicated that compound **5** could be a promising IRAK4 inhibitor for the treatment of mutant MYD88 DLBCL.

Key words: Interleukin-1 receptor associated kinase 4; Imidazo[1,2-*b*]pyridazine; Diffuse large B-cell lymphoma; Drug design; Antitumor agents

Introduction

Diffuse large B-cell lymphoma (DLBCL) is the most common lymphoma subtype representing roughly 30-35% of all non-Hodgkin lymphomas case.[1] Based on the gene expression profiling DLBCL could be divided into two major molecular subtypes termed germinal center B-cell-like (GCB) and activated B-cell-like (ABC) which has a poor prognosis.[2] ABC-DLBCL is addicted to constitutive B-cell receptor (BCR) signaling and NF- κ B activation rendering them sensitive to Bruton's tyrosine kinase (BTK) inhibitors ibrutinib.[3, 4] However, harboring MYD88 L265P variant which provides an alternative pathway to activate NF- κ B was found to convey resistance to ibrutinib in BCR-independent patients,[5] and this recurrent gain of function mutation occurred in 29% of ABC-DLBCL patients.[6] Therefore, novel therapeutic drugs need to be developed to tackle this urgent problem.

IRAK4 is an essential effector to promote tumor progression in MYD88 L265P mutated DLBCL.[6] Mutated MYD88 protein induces dimerization of IRAK4 via death domain and initiates trans-autophosphorylation of IRAK4 without external ligands stimulation.[7, 8] Subsequently, it triggers the allosteric activation of IRAK1,[7] phosphorylation of the IKK β which resulting in the degeneration of I κ B and constitutive NF- κ B activation.[8-10] Recently, Zhang et al. reported that downregulation of phosphorylated IRAK4 and NF- κ B could disrupt tumor–stroma IL-1 β -IRAK4 feedforward circuitry and increase chemotherapeutic efficacy in PDAC.[11, 12] Remarkably, individuals who lack IRAK4 show only increased susceptibility to certain pyogenic infections without extensive viral or fungal infection risk prior to adolescence.[13, 14] These suggest that IRAK4 is a promising anti-tumor target and selective IRAK4 inhibitors may have anti-neoplastic activity while avoiding severe side effect.

In the past decade, small molecule IRAK4 inhibitors of various chemotypes have been described and reviewed,[15, 16] with notable contributions from groups including Pfizer,[17] Curis,[18]

BMS,[19, 20] Nimbus,[21] AstraZeneca,[22, 23] and Genentech[24] (Figure 1). It has been reported that, in pyrazolo[1,5-*a*]pyrimidine IRAK4 inhibitors, an intramolecular hydrogen bond between the amide N-H and pyrimidine nitrogen stabilizes the structure into a planar conformation that allows for a favorable slanted face-to-edge π - π interaction with the gatekeeper Tyr262 and moreover pyrazolo[1,5-*a*]pyrimidine moiety binds to the hinge region effectively through the backbone of Met265 and Val263 via the amide carbonyl and the unusual C2 hydrogen. [24-26] Given that potential selectivity issues of the pyrazolo[1,5-*a*]pyrimidine scaffold,[27] a series of new IRAK4 inhibitors were designed through scaffold-hopping strategy (Figure 2). We retained all of the intra- and intermolecular interactions between pyrazolo[1,5-*a*]pyrimidine moiety and IRAK4 to afford imidazo[1,2-*b*]pyridazine scaffold. Meanwhile, in consideration of the atypical hydrogen bond provided by C2 hydrogen of pyrazole ring, we designed an imidazo[1,5-*a*]pyrimidine scaffold to determine whether integrated “hinge binding element” was essential to IRAK4 potency (Figure 2). Most of IRAK4 inhibitors described in the literature were focused on anti-inflammatory and autoimmune disease, but few of IRAK4 inhibitors involved in the treatment of DLBCL were reported. Herein, we reported a series of imidazo[1,2-*b*]pyridazines as IRAK4 inhibitors focusing on the application of the treatment of DLBCL.

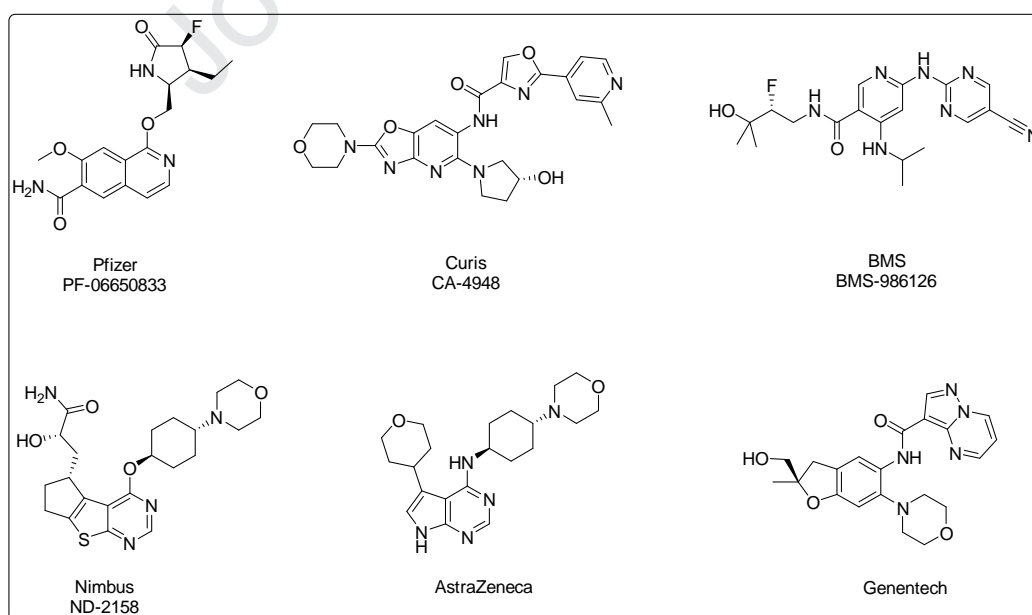


Figure 1. Representative small molecule inhibitors of IRAK4.

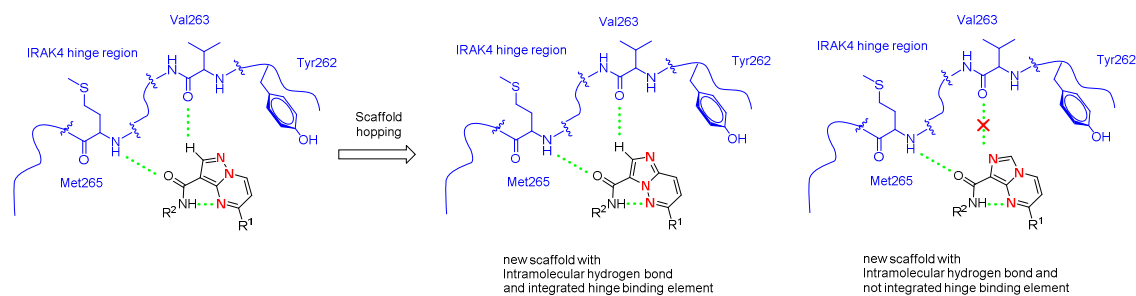


Figure 2. Rational design of target compounds by scaffold hopping strategy.

Results and Discussion

Enzymatic activity and cytotoxicity assay of alternative scaffold representations

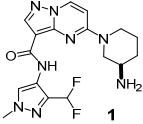
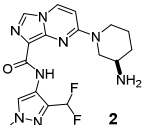
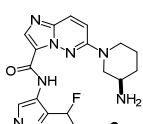
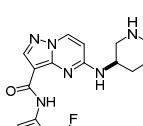
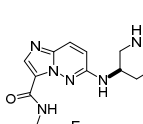
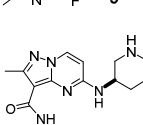
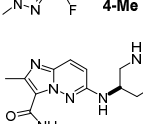
All alternative scaffold representations listed in Table 1 were evaluated for IRAK4 inhibitory potency using Z-lyte kinase assay. After optimizing the Ser/Thr protein kinase detection platform, IC_{50} values of these compounds were determined by inhibition rate curve of various dosages. As is shown in Table 1, the imidazo[1,2-*b*]pyridazine derivatives (compounds **3** and **5**) showed equal potency (IC_{50} = 8.7 nM and 1.3 nM, respectively) to their counterparts pyrazolo[1,5-*a*]pyrimidines (compounds **1** and **4**) against IRAK4. The imidazo[1,5-*a*]pyrimidine derivative **2** characterized by nitrogen atom at the 2-position, completely lost activity compared to compounds **1** and **3**, indicating that C2 proton from pyrazole or imidazole ring was vital to retain IRAK4 potency. Corresponding methylated derivatives of **4** and **5** at C2 position (compounds **4-Me** and **5-Me**) exhibited significant loss of IRAK4 potency compared to compounds **4** and **5**. It further confirmed that the importance of the C2 proton from pyrazole or imidazole ring.

These compounds were also tested cytotoxicity against DLBCL cell lines *in vitro* (Table 1). Compound **5** selectively suppressed OCI-LY10 and TMD8 cells with MYD88 L265P mutation (IC_{50} = 0.7 μ M and 1.2 μ M, respectively), but not Ramos and HT cell lines with WT MYD88 (IC_{50} = 11.4 μ M and 40.1 μ M, respectively). Whereas compound **4** inhibited all cells mentioned above without selectivity presumably due to the potential off-target toxicity. These results indicated that compound **5** possessed higher target selectivity and less toxicity than **4**.

Based on the excellent IRAK4 potency and selective cytotoxicity of **5**, imidazo[1,2-*b*]pyridazine scaffold represented an exciting start point for the development of a novel IRAK4 inhibitor against ABC DLBCL.

Table 1

Enzymatic activity and cytotoxicity assay of alternative scaffold representations.

Compd	IRAK4 IC ₅₀ (nM) ^[a]	OCI-LY10 IC ₅₀ (μM) ^[a]	TMD8 IC ₅₀ (μM) ^[a]	Ramos IC ₅₀ (μM) ^[a]	HT IC ₅₀ (μM) ^[a]
 1	9.3 ± 2.5	5.5 ± 0.4	7.3 ± 2.4	19.0 ± 8.5	29.2 ± 6.9
 2	> 1000	> 50	> 50	> 50	> 50
 3	8.7 ± 1.0	10.7 ± 2.1	17.8 ± 6.1	44.3 ± 6.8	41.7 ± 1.8
 4	2.5 ± 0.8	0.2 ± 0.0	0.2 ± 0.0	0.6 ± 0.0	2.7 ± 0.7
 5	1.3 ± 0.1	0.7 ± 0.1	1.2 ± 0.4	11.4 ± 3.8	40.1 ± 7.1
 4-Me	> 1000	NT ^[b]	NT ^[b]	NT ^[b]	NT ^[b]
 5-Me	> 1000	NT ^[b]	NT ^[b]	NT ^[b]	NT ^[b]

[a] Data are the mean ± SD of at least three independent experiments.

[b] NT represents for no test.

SARs of imidazo[1,2-*b*]pyridazines and cellular activity evaluation

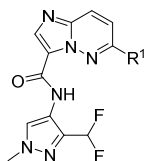
The modification of compound **5** was first focused on replacement of (3*R*)-3-aminopiperidine moiety with various amines, and compounds **6-13** was obtained (Table 2). Biological results suggested that *R*-configuration in **5** was important for maintaining IRAK4 inhibitory potency, and the *S*-isomer **6** displayed a 10-fold less potency against IRAK4. The 5-membered ring (**7**, IRAK4 IC₅₀ = 7.7 nM) and 7-membered ring (**9**, IRAK4 IC₅₀ = 9.0 nM) exhibited minimal decrease in

potency, which indicated the size of the ring influences slightly the activity. Nevertheless, compound **8** lost potency completely, suggesting that the 5-membered ring compared to 6-membered ring may have different SARs. The position of amino in aminopiperidine group is vital to IRAK4 inhibitory potency. The 4-substituted analogue **10** resulted in almost 10-fold loss of potency. In addition, replacement of (3*R*)-3-aminopiperidine group (**5**) with a piperazine group (**12**) displayed 20-fold loss of potency. Although a tertiary amine attached to the scaffold (**3**) could be tolerated, the (3*R*)-3-methylaminopiperidine analogue (**13**) showed a complete loss of potency. Throughout the SAR studies, compound **5** still showed highest potency.

Then SARs of pyrazole moiety were investigated. Compared with **5**, substituents with trifluoromethyl (**14**), cyan (**15**), and formamide (**16**) were 7-, 12-, and 4-fold less potent, respectively. Replacing the difluoromethyl group with a methyl (**17**) resulted in dramatic reduction in potency, suggesting that the electron-withdrawing groups in pyrazole moiety could be beneficial for IRAK4 potency. Modifications of the trifluoromethyl-pyrazole **14**, selected for synthetic feasibility over difluoromethyl-pyrazole **5**, were then undertaken to investigate the vectors to the solvent front region. All of the compounds demonstrated disappointing results. The potency decreased with larger substituents toward solvent (**18** and **19**). When hydrophilic groups 4-piperidyl (**20**) and 4-tetrahydropyranyl (**21**) were introduced to pyrazole moiety, IRAK4 potency was eroded presumably due to steric clash with the IRAK4. Through the thorough investigation of SARs, we found that **5** remained the most effective IRAK4 inhibitor.

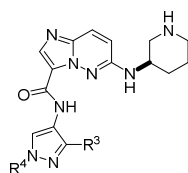
We subsequently selected potent compounds in enzymatic assays to assess their cell killing ability against DLBCL cell lines *in vitro* (Table 4). All of these compounds displayed selective cytotoxicity against MYD88 L265P mutation cell lines, OCI-LY10 and TMD8, without obvious cytotoxicity against Ramos and HT cell lines. Among these compounds, the IC₅₀ values of **9** (OCI-LY10 IC₅₀ = 0.8 μM and TMD8 IC₅₀ = 1.2 μM) showed a similar level to **5**.

The binding model of **5** with IRAK4 was predicted by Glide docking in Schrodinger (Figure 3). The results suggested that compound **5** could insert ATP pocket of IRAK4 deeply and form a single hydrogen bond interaction provided by the amide oxygen with Met265 of the hinge region. The (3*R*)-3-aminopiperidine group, occupying the ATP ribose pocket, donates extensive hydrogen-bonding interaction to Asp329, Asn316, and Ala315. The computational modeling results might explain the excellent enzyme potency of compound **5**.

Table 2SAR of imidazo[1,2-*b*]pyridazines **3** and **5-13**.

Compd	R ¹	IRAK4 IC ₅₀ (nM) ^[a]
3		8.7 ± 1.0
5		1.3 ± 0.1
6		36.2 ± 7.2
7		7.7 ± 1.3
8		> 1000
9		9.0 ± 1.3
10		80.3 ± 42.3
11		17.5 ± 4.5
12		65.5 ± 26.7
13		> 1000

[a] Data are the mean ± SD of at least three independent experiments.

Table 3SAR of imidazo[1,2-b]pyridazines **5** and **14-21**.

Compd	R ³	R ⁴	IRAK4 IC ₅₀ (nM) ^[a]
5	CHF ₂	Me	1.3 ± 0.1
14	CF ₃	Me	23.5 ± 13.0
15	CN	Me	40.8 ± 24.5
16	CONH ₂	Me	12.5 ± 4.8
17	Me	Me	> 1000
18	CF ₃	Et	32.3 ± 18.4
19	CF ₃	i-Pr	77.0 ± 41.3
20	CF ₃	4-piperidyl	52.2 ± 34.1
21	CF ₃	4-THP	49.7 ± 24.5

[a] Data are the mean ± SD of at least three independent experiments.

Table 4

Cytotoxicity assay of potent compounds.

Compd	OCI-LY10 IC ₅₀ (μM) ^[a]	TMD8 IC ₅₀ (μM) ^[a]	Ramos IC ₅₀ (μM) ^[a]	HT IC ₅₀ (μM) ^[a]
6	22.3 ± 3.8	22.3 ± 8.0	> 50	> 50
7	3.6 ± 0.5	8.3 ± 2.9	45.0 ± 4.6	> 50
9	0.8 ± 0.1	1.2 ± 0.4	7.2 ± 1.6	35.9 ± 3.1
11	8.8 ± 1.0	17.7 ± 5.1	> 50	> 50
14	2.8 ± 0.3	5.9 ± 2.4	> 50	> 50
15	5.8 ± 0.1	14.8 ± 6.0	28.8 ± 11.1	> 50
18	3.6 ± 0.5	6.1 ± 2.8	> 50	> 50
21	10.5 ± 1.2	11.1 ± 4.5	> 50	> 50

[a] Data are the mean ± SD of at least three independent experiments.

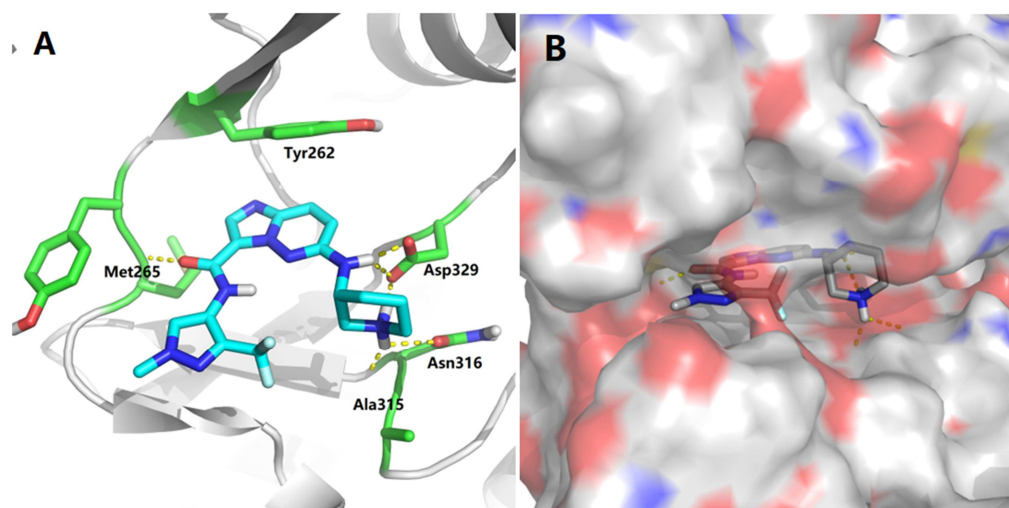


Figure 3. Binding-mode analysis of **5** with IRAK4 (PDB code: 4Y73). (A) The (3*R*)-3-aminopiperidine moiety donated extensive hydrogen-bonding interaction to ATP pocket. (B) The difluoromethyl-pyrazole moiety extended to solvent and the (3*R*)-3-aminopiperidine moiety occupied ribose binding region of the ATP pocket.

Selectivity profiling of compounds **5** and **4**

We further investigated the kinase selectivity profile of compounds **5** and **4** against a panel of kinases (Figure 4). At the concentration of 0.1 μM , **5** showed less than 50% inhibition against most of tested kinases, and displayed greater than 50% inhibition in only three kinases, including FLT3, FLT3-ITD and c-Kit. These three kinases have been reported to be crucial in the development of acute myeloid leukemia (AML), indicating a potential indication of these structures.[9] By comparison, compound **4** showed more than 50% inhibition against eight kinases, including FLT3, FLT3-ITD, c-Kit, RET, SRC, VEGFR3, VEGFR2, and ABL. These data demonstrated that compound **5** possessed much higher selectivity than **4**, which was consistent with the more selective anti-proliferation function of **5** against tumor cells than **4**.

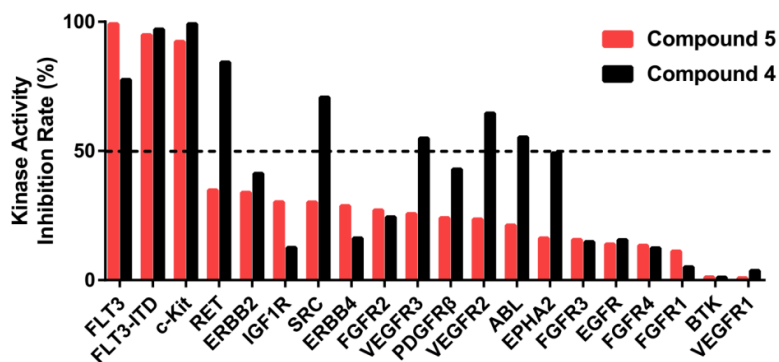


Figure 4. Selectivity profiling of compounds **5** and **4** against a panel of kinases. Inhibitory activities of the compounds (at the concentration of 0.1 μ M) against these kinases were determined by using ELISA assay.

Compound 5 inhibits the viability of DLBCL cells by targeting IRAK4 signaling

To test whether the anti-tumor function of these IRAK4 inhibitors through inhibiting IRAK4 and downstream signaling activation, we conducted Western blot analysis of OCI-LY10 and TMD8 cell lines by incubating with or without compound **5** at indicated concentrations for 2h. The results showed that compound **5** dose-dependently decreased the autophosphorylation of IRAK4 (Thr-345/Ser-346) compared to vehicle control in OCI-LY10 cells (Figure 5A, B). Moreover, the phosphorylation of downstream molecules, IKK β and NF- κ B transcription factor (p65), could also be effectively blocked upon compound **5** treatment. The inhibitory effect on IRAK4 and its downstream signaling in TMD8 cells was also examined, and similar results were observed (Figure 5C, D). These results indicated that compound **5** inhibited DLBCL cells by targeting IRAK4 signaling.

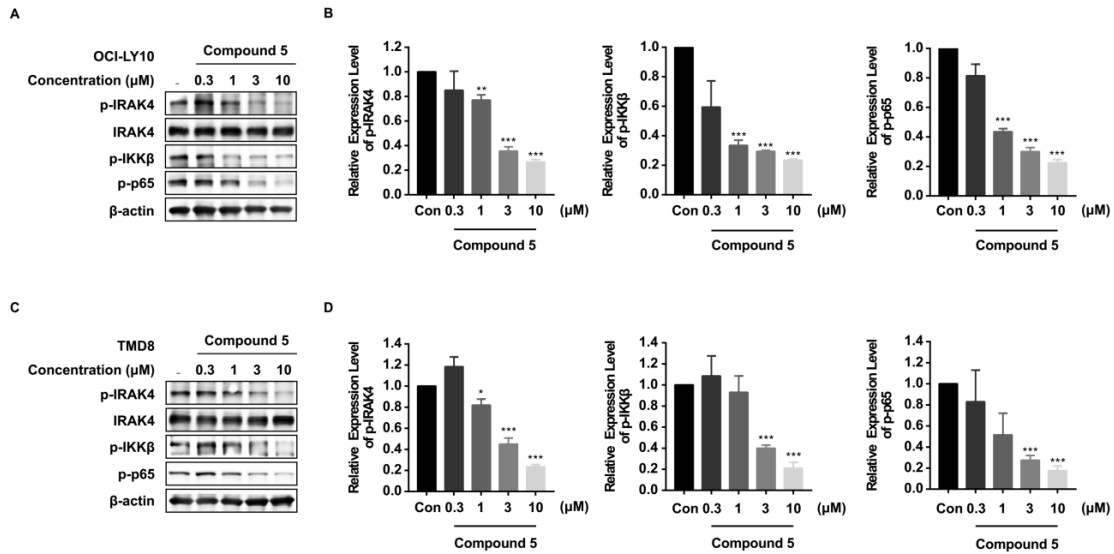


Figure 5. Compound 5 effectively inhibited the phosphorylation of IRAK4 and the activation of downstream effectors IKK β and p65 in OCI-LY10 (A, B) and TMD8 (C, D) cells. All protein samples treated with compound 5 or DMSO were collected after two hours incubation and analyzed by Western blot. Protein quantitative data of p-IRAK4, p-IKK β and p-p65 were analyzed with Image J. Significance threshold was fixed at * $p < 0.05$, ** $p < 0.01$, *** $p < 0.001$.

Combination of compound 5 with ibrutinib synergistically exhibits anti-tumor activity to DLBCL cells

Previous study proved that combination of IRAK4 inhibitor and BTK inhibitor synergistically decreased the cell viability in cells harboring gain-of-function MYD88 L265P mutation.[23] Hence, we treated the BCR-dependent TMD8 cells with compound 5 and ibrutinib at different concentrations for 72 h. The result showed that this combination strategy exhibited synergistic anti-tumor effects against TMD8 cells compared to each treatment alone (Figure 6). According to the combination index (CI) value obtained by the CalcuSyn software,[28] we found that combining compound 5 at 0.3 μM with ibrutinib at 6.3 nM exerted maximum synergistic response against TMD8 cells growth with CI of 0.13 (Figure 6). These results revealed that IRAK4 is a promising drug target for DLBCL treatment and the combined use of ibrutinib and IRAK4 inhibitors will obtain more benefits in future clinical utilization.

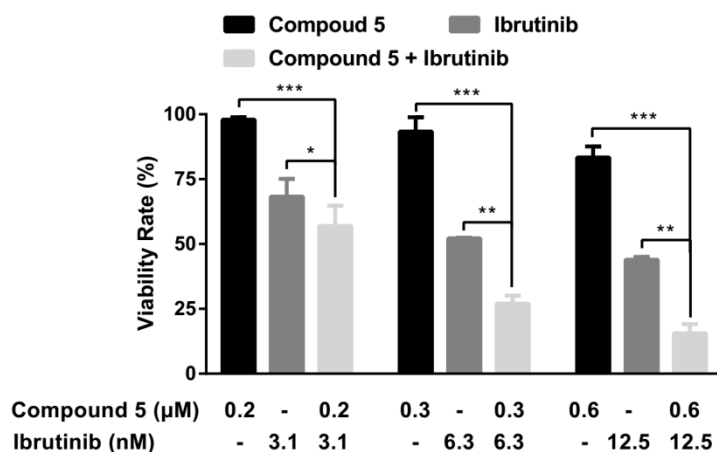


Figure 6. Synergistic anti-tumor efficacy of compound **5** and BTK inhibitor ibrutinib in MYD88 L265P⁺ TMD8 cells. Cells were incubated with various doses of ibrutinib and compound **5** for 72 h. Experiment was conducted by at least three times and all data were represented as mean \pm SD. Statistical significance was analyzed by Student's *t*-test. * $P < 0.05$, ** $P < 0.01$, *** $P < 0.001$.

Chemistry

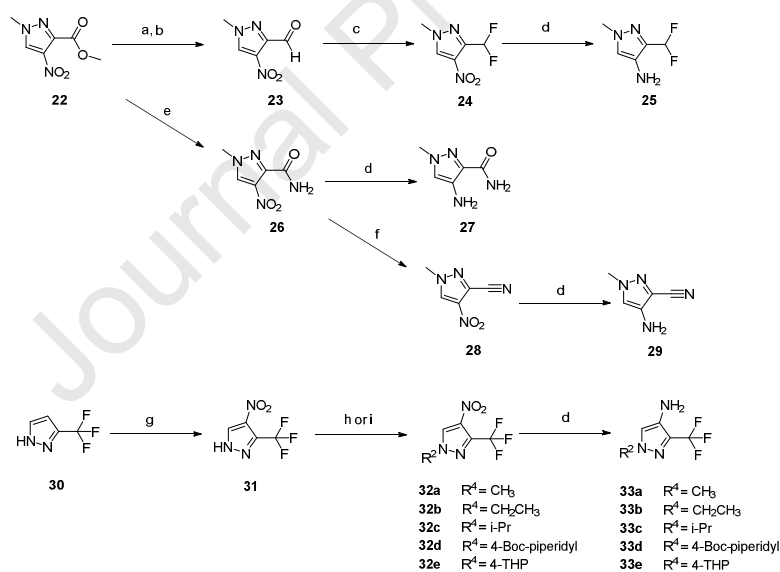
These key intermediates **25**, **27**, **29**, and **33a-33e** were prepared as shown in Scheme 1. Both of intermediates **25**, **27**, and **29** were synthesized from methyl 1-methyl-4-nitro-1*H*-pyrazole-3-carboxylate (**22**), which have been previously disclosed.[25] Nitration of 3-(trifluoromethyl)-1*H*-pyrazole (**30**) with fuming nitric acid provided 4-nitro-3-(trifluoromethyl)-1*H*-pyrazole **31**. Then nucleophilic substitution between **31** and iodoalkanes resulted in **32a-32c**. It could not get corresponding **32d-32e** directly through nucleophilic substitution with iodide of 4-Boc-piperidyl and 4-THP. Then *p*-toluenesulfonate of 4-Boc-piperidyl and 4-THP was used to react with **31**, and **32d-32e** was afforded. Hydrogenation of **32a-32e** nitro group with Pd/C delivered intermediates **33a-33e**.

The general synthetic route toward **3** and **5-21** was depicted in Scheme 2. An Aldol condensation between 6-chloropyridazin-3-amine (**34**) and *N,N*-dimethylformamide dimethyl acetal yielded compound **35**. Nucleophilic aromatic substitution of **35** with ethyl bromoacetate followed by ring closure provided ethyl 6-chloroimidazo[1,2-*b*]pyridazine-3-carboxylate (**36**). The 6-methoxyimidazo[1,2-*b*]pyridazine-3-carboxylic acid instead of intermediate **37** was obtained when **36** was hydrolyzed with LiOH in methanol/tetrahydrofuran/water, and intermediate **37** was obtained in the mixed solvent without methanol. Subsequent condensation of **37** with

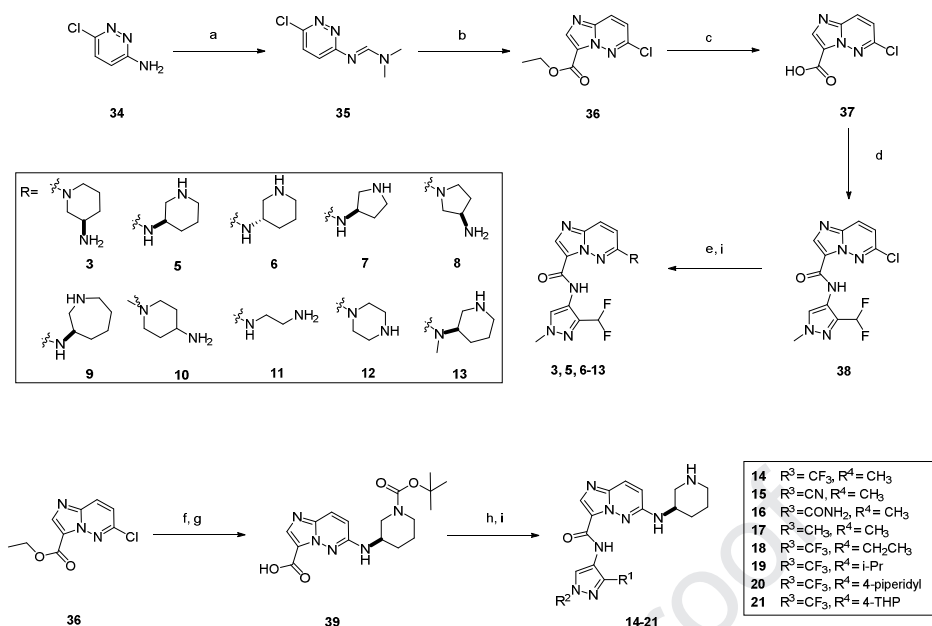
intermediate **25** provided key intermediate **38**, which was converted to corresponding target compounds **3**, **5**, and **6-13** through electrophilic aromatic substitution and subsequent deprotection. Compound **39** was synthesized by the S_NAr and hydrolysis reaction from **36**. Likewise, condensation of **39** with corresponding intermediates **33a-33e** and subsequent deprotection afforded target compounds **14-21**.

Electrophilic aromatic substitution of **40** with *tert*-butyl (3*R*)-3-aminopiperidine-1-carboxylate and hydrolysis provided carboxylic acid **41**. Then condensation of intermediate **41** with **25** and subsequent deprotection delivered target compound **2**. Target compounds **1** and **4** could be afforded through similar processes (Scheme 3).

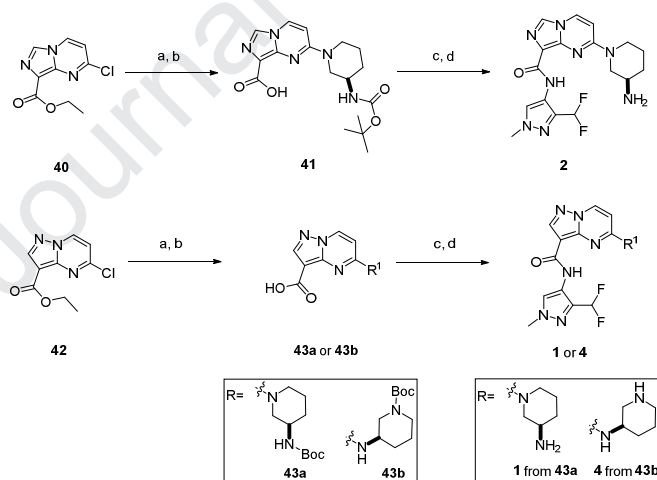
Through similar synthetic process of **4** and **5**, compounds **4-Me** and **5-Me** could be synthesized from ethyl 5-chloro-2-methylpyrazolo[1,5-*a*]pyrimidine-3-carboxylate **44** and ethyl 6-chloro-2-methylimidazo[1,2-*b*]pyridazine-3-carboxylate **46** respectively (Scheme 4).



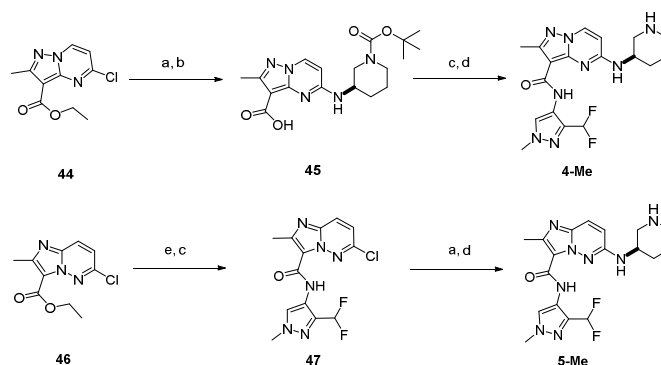
Scheme 1. Synthesis of Intermediates **25**, **27**, **29**, and **33a-33e**: a) DIBALH, DCM, 0 °C to rt; b) IBX, DMSO, rt; (c) DAST, DCM, -40 °C to rt; d) H₂, Pd/C, MeOH, rt; e) NH₃/MeOH, 50 °C, sealed tube; f) POCl₃, DIPEA, 0 °C to rt; g) Fuming HNO₃/H₂SO₄, 0 °C to rt; h) tetrahydro-2*H*-pyran-4-yl 4-methylbenzenesulfonate or *tert*-butyl 4-(tosyloxy)piperidine-1-carboxylate, Cs₂CO₃, DMF, 70 °C; i) iodoalkane, K₂CO₃, DMF, rt.



Scheme 2. Synthesis of target compounds **3** and **5-21**: a) *N,N*-dimethylformamide dimethyl acetal, 100 °C; b) i. ethyl bromoacetate, MeCN, 85 °C; ii. DIPEA, rt; c) LiOH·H₂O, THF/H₂O, 35 °C; d) intermediate **25**, EDCI, HOBT, DIPEA, DMF, rt; e) amines, KF, DIPEA, DMSO, 100 °C; f) *tert*-butyl (3*R*)-3-aminopiperidine-1-carboxylate, KF, DMSO, 100 °C; g) LiOH·H₂O, MeOH/THF/H₂O, 30 °C; h) intermediates **27**, **29** and **33a-e**, EDCI, HOBT, DIPEA, DMF, rt; i) TFA, DCM, rt.



Scheme 3. Synthesis of target compounds **1**, **2**, and **4**: a) *tert*-butyl (3*R*)-3-aminopiperidine-1-carboxylate or *tert*-butyl (*R*)-3-aminopiperidine-1-carboxylate, KF, DMSO, 100 °C; b) LiOH·H₂O, MeOH/THF/H₂O, 50 °C; c) intermediate **25**, HATU, DIPEA, MeCN, rt; d) TFA, DCM, rt.



Scheme 4. Synthesis of target compounds **4-Me** and **5-Me**: a) *tert*-butyl (*R*)-3-aminopiperidine-1-carboxylate, KF, DMSO, 100 °C; b) LiOH·H₂O, MeOH/THF/H₂O, 50 °C; c) intermediate **25**, HATU, DIPEA, MeCN, rt; d) TFA, DCM, rt; e) LiOH·H₂O, THF/H₂O, 35 °C.

Conclusion

In summary, we designed and synthesized a series of imidazo[1,2-*b*]pyridazine IRAK4 inhibitors and analyzed SARs. Among these compounds, **3**, **5**, **7**, and **9** showed superior IRAK4 inhibitory activity and cytotoxicity against MYD88 L265P mutation cell lines. In particular, compound **5** displayed excellent IRAK4 potency ($IC_{50} = 1.3$ nM) and 10-fold greater selectivity on MYD88 L265P mutation cell lines (OCI-LY10 $IC_{50} = 0.7$ μ M and TMD8 $IC_{50} = 1.2$ μ M) than WT MYD88 cell lines. Besides, compound **5** demonstrated a favorable selectivity profile and only three kinases (FLT3, FLT3-ITD, and c-Kit) were observed for > 50% inhibition rate. Considering selectivity profile of **5**, it displayed cellular selectivity for ABC-DLBCL with MYD88 mutation in cytotoxicity assay consequently. Western blot assay showed that compound **5** could inhibit the phosphorylation of IKK β and activation of NF- κ B in OCI-LY10 and TMD8 cell lines. Finally, inhibition of NF- κ B activity translated to synergistic effect on the loss of cell viability in TMD8 cells treated with a combination of compound **5** and ibrutinib. These results demonstrated that compound **5** could be a promising IRAK4 inhibitor and worthy of further investigation for the treatment of mutant MYD88 DLBCL.

Experimental Section

Chemistry

All purchased solvents and chemicals were used without further purification unless otherwise noted. Flash chromatography was performed using silica gel (300-400 mesh). All reactions were

monitored by thin layer chromatography (TLC) or high performance liquid chromatography. ^1H NMR and ^{13}C NMR were generated in CDCl_3 , $\text{DMSO}-d_6$, or CD_3OD on Varian Mercury 300, 400, or 500 NMR spectrometers. Mass spectrometry was conducted using an Agilent 6110 Quadrupole LC/MS (ESI-MS mode). High resolution mass spectrometry was conducted using an Agilent G6520 Q-TOF spectrometer (ESI-MS mode). The purity of all tested compounds was determined by the Agilent infinity 1260 HPLC system coupled with a diode array detector (DAD) and the Eclipse Plus C18 column (4.6 \times 150 mm, 5 μm).

(R)-5-(3-aminopiperidin-1-yl)-N-(3-(difluoromethyl)-1-methyl-1H-pyrazol-4-yl)pyrazolo[1,5-a]

pyrimidine-3-carboxamide trifluoroacetate (1): A solution of ethyl 5-chloropyrazolo[1,5-a]pyrimidine-3-carboxylate **42** (569 mg, 2.52 mmol), *tert*-butyl (*R*)-piperidin-3-ylcarbamate (909 mg, 4.54 mmol) and potassium fluoride (1.47 g, 25.2 mmol) was stirred at 100 $^\circ\text{C}$ for 2 h. The mixture was allowed to cool to room temperature and H_2O was added upon which precipitate formed. The precipitate was filtered off and washed with water and dried to afford the white solid. Then the solid dissolved in methanol/tetrahydrofuran/water (6 mL/6 mL/2 mL), followed by addition of lithium hydroxide monohydrate (527 mg, 12.6 mmol) was stirred overnight at 50 $^\circ\text{C}$ for 2 h. The solvent was removed in vacuo. The residue was added water (4 mL) and adjusted pH to 3-4 with 1 mol/L hydrochloric acid upon which precipitate formed. The precipitate was filtered off, washed with water and dried to afford compound **43a** as a pale yellow solid (800 mg, 88%). ^1H NMR (400 MHz, Chloroform-*d*) δ 8.44–8.18 (m, 2H), 6.56 (d, J = 8.0 Hz, 1H), 4.64 (s, 1H), 3.97 (s, 2H), 3.66 (s, 2H), 3.48 (d, J = 12.9 Hz, 1H), 2.04 (d, J = 11.0 Hz, 1H), 1.86 (s, 1H), 1.67 (dd, J = 27.6, 11.4 Hz, 2H), 1.44 (s, 9H). MS (ESI): 360.3 [M -H].

A solution of **43a** (75 mg, 0.217 mmol), intermediate **25** (35 mg, 0.228 mmol), EDCI (48 mg, 0.249 mmol), HOBT (34 mg, 0.249 mmol) and *N,N*-diisopropylethylamine (80 μL , 0.484 mmol) in DMF (2 mL) was stirred overnight at room temperature. The reaction was taken up in ethyl acetate, washed with water and brine. The organic phase was dried over anhydrous sodium sulfate, filtered, and concentrated. The residue was purified by prep-TLC (5% MeOH in DCM) to afford *tert*-butyl (*R*)-(1-(3-((3-(difluoromethyl)-1-methyl-1H-pyrazol-4-yl)carbamoyl)pyrazolo[1,5-a]

pyrimidin-5-yl)piperidin-3-yl)carbamate (42 mg, 41%). Then it dissolved in dichloromethane (4 mL) which was added trifluoroacetic acid (1 mL). The mixture was stirred at room temperature for 2 h. The solvent was removed under reduced pressure and the residue was purified by triturating with methanol/diethyl ether (1 mL/5 mL) to afford compound **1** as a white solid (28 mg, 65%). ^1H NMR (400 MHz, DMSO- d_6) δ 9.36 (s, 1H), 8.88 (d, J = 7.9 Hz, 1H), 8.33 (d, J = 15.8 Hz, 2H), 8.06 (s, 3H), 7.10 (t, J = 53.9 Hz, 1H), 6.82 (d, J = 7.9 Hz, 1H), 4.15 (d, J = 14.0 Hz, 2H), 3.88 (s, 3H), 3.56 (t, J = 10.8 Hz, 2H), 2.11–1.98 (m, 1H), 1.91–1.77 (m, 1H), 1.77–1.52 (m, 2H). ^{13}C NMR (126 MHz, DMSO- d_6) δ 158.97, 156.60, 145.49, 137.13, 133.43 (t, J = 27.3 Hz), 124.47, 118.50, 112.82 (t, J = 229.4 Hz), 100.23, 98.10, 47.67, 46.42, 43.98, 27.62, 21.48. ESI-HRMS m/z [$M+H$] $^+$ calcd for $\text{C}_{17}\text{H}_{21}\text{F}_2\text{N}_8\text{O}$: 391.1801, found: 391.1792.

(*R*)-2-(3-aminopiperidin-1-yl)-*N*-(3-(difluoromethyl)-1-methyl-1*H*-pyrazol-4-yl)imidazo[1,5-*a*]

pyrimidine-8-carboxamide trifluoroacetate (2): A solution of ethyl 2-chloroimidazo[1,5-*a*]pyrimidine-8-carboxylate **40** (366 mg, 1.62 mmol), *tert*-butyl (*R*)-piperidin-3-ylcarbamate (585 mg, 2.92 mmol) and potassium fluoride (942 mg, 16.2 mmol) was stirred at 100 °C for 2 h. The mixture was allowed to cool to room temperature and H_2O was added upon which precipitate formed. The precipitate was filtered off and washed with water and dried to afford the white solid. Then the solid dissolved in methanol/tetrahydrofuran/water (8 mL/8 mL/3.5 mL), followed by addition of lithium hydroxide monohydrate (680 mg, 16.2 mmol) was stirred at 50 °C overnight. The solvent was removed in vacuo. The residue was added water (5 mL) and adjusted pH to 3-4 with 1 mol/L hydrochloric acid upon which precipitate formed. The precipitate was filtered off, washed with water and dried to afford compound **41** as a pale yellow solid (467 mg, 80%). ^1H NMR (300 MHz, DMSO- d_6) δ 11.20 (s, 1H), 8.57–8.42 (m, 1H), 7.91 (dd, J = 3.8, 2.2 Hz, 1H), 7.01 (d, J = 6.8 Hz, 1H), 6.76 (d, J = 7.8 Hz, 1H), 4.12 (s, 2H), 3.48–3.21 (m, 2H overlapped with H_2O) 3.13 (s, 1H), 1.82 (d, J = 18.8 Hz, 2H), 1.58–1.45 (m, 2H), 1.39 (t, J = 3.0 Hz, 9H). MS (ESI): 360.3 [$M-H$] $^-$.

A solution of **41** (100 mg, 0.277 mmol), intermediate **25** (37 mg, 0.251 mmol), HATU (192 mg, 0.503 mmol) and *N,N*-diisopropylethylamine (105 μL , 0.629 mmol) in acetonitrile (5 mL) was stirred for 2 h at room temperature. The reaction was taken up in ethyl acetate, washed with water and brine. The organic phase was dried over anhydrous sodium sulfate, filtered, and

concentrated. The residue was purified by flash column chromatography eluting with 1% to 3% MeOH in DCM to afford *tert*-butyl(*R*)-(1-(8-((3-(difluoromethyl)-1-methyl-1*H*-pyrazol-4-yl) carbamoyl)imidazo[1,5-*a*]pyrimidin-2-yl)piperidin-3-yl)carbamate (45 mg, 36%). Then it dissolved in dichloromethane (4 mL) which was added trifluoroacetic acid (1 mL). The mixture was stirred at room temperature for 2 h. The solvent was removed under reduced pressure and the residue was purified by triturating with diethyl ether (1 mL/5 mL) to afford compound **2** as a white solid (31 mg, 67%). ¹H NMR (300 MHz, DMSO-*d*₆) δ 9.39 (s, 1H), 8.61 (d, *J* = 7.9 Hz, 1H), 8.33 (s, 1H), 8.24–8.06 (m, 3H), 8.05 (s, 1H), 7.10 (t, *J* = 54.0 Hz, 1H), 6.82 (d, *J* = 8.0 Hz, 1H), 4.22 (d, *J* = 13.6 Hz, 1H), 4.05 (s, 2H), 3.87 (s, 3H), 3.87 (s, 3H), 3.49 (dd, *J* = 13.3, 8.2 Hz, 2H), 2.02 (d, *J* = 7.0 Hz, 1H), 1.82 (s, 1H), 1.76–1.52 (m, 2H). ¹³C NMR (126 MHz, DMSO-*d*₆) δ 159.00, 155.18, 139.24, 133.32 (t, overlapped), 133.15, 125.62, 124.09, 118.92, 115.17, 112.80 (t, *J* = 229.7 Hz), 47.39, 46.42, 44.09, 27.70, 21.59. ESI-HRMS *m/z* [*M*+H]⁺ calcd for C₁₇H₂₁F₂N₈O: 391.1801, found: 391.1807.

(*R*)-6-(3-aminopiperidin-1-yl)-*N*-(3-(difluoromethyl)-1-methyl-1*H*-pyrazol-4-yl)imidazo[1,2-*b*]

pyridazine-3-carboxamide (3): This compound was prepared from *tert*-butyl (*R*)-piperidin-3-ylcarbamate as described in the synthesis of **8** as an off-white solid (78%). ¹H NMR (300 MHz, DMSO-*d*₆) δ 9.99 (s, 1H), 8.38 (s, 1H), 8.29–7.94 (m, 5H), 7.37 (d, *J* = 10.1 Hz, 1H), 7.31 (s, 1H), 3.98 (s, 1H), 3.91 (s, 3H), 3.77 (s, 1H), 3.51–3.27 (m, 3H), 2.10–1.95 (m, 1H), 1.94–1.78 (m, 1H), 1.78–1.55 (m, 2H). ¹³C NMR (126 MHz, DMSO-*d*₆) δ 155.46, 155.26, 138.11, 137.64, 134.50 (t, *J* = 26.8 Hz), 127.06, 125.83, 121.46, 117.25, 113.02, 112.29 (t, *J* = 230.9 Hz), 49.78, 46.46, 45.32, 28.30, 21.32. ESI-HRMS *m/z* [*M*+H]⁺ calcd for C₁₇H₂₁F₂N₈O: 391.1801, found: 391.1790.

(*R*)-*N*-(3-(difluoromethyl)-1-methyl-1*H*-pyrazol-4-yl)-5-(piperidin-3-ylamino)pyrazolo[1,5-*a*]

pyrimidine-3-carboxamide trifluoroacetate (4): This compound was prepared from *tert*-butyl (*R*)-3-aminopiperidine-1-carboxylate as described in the synthesis of **1** as an off-white solid (72%). ¹H NMR (300 MHz, DMSO-*d*₆) δ 9.27 (s, 1H), 8.86–8.53 (m, 3H), 8.26 (d, *J* = 7.0 Hz, 2H), 8.18 (d, *J* = 7.1 Hz, 1H), 7.11 (t, *J* = 54.2 Hz, 1H), 6.48 (d, *J* = 7.7 Hz, 1H), 4.41 (s, 1H), 3.88 (s, 3H), 3.20 (s, 2H), 3.10 (s, 2H), 1.99 (d, *J* = 9.9 Hz, 2H), 1.88–1.58 (m, 2H). ¹³C NMR (126 MHz, DMSO-*d*₆) δ 159.21, 156.45, 145.86, 144.80, 136.30, 134.02 (t, *J* = 28.7 Hz), 125.01, 118.36, 115.74, 112.73 (t, *J* =

230.7 Hz), 101.65, 100.66, 45.36, 43.22, 42.97, 26.91, 18.89. ESI-HRMS m/z $[M+H]^+$ calcd for $C_{17}H_{21}F_2N_8O$: 391.1801, found: 391.1793.

(*R*)-*N*-(3-(difluoromethyl)-1-methyl-1*H*-pyrazol-4-yl)-6-(piperidin-3-ylamino)imidazo[1,2-*b*]

pyridazine-3-carboxamide trifluoroacetate (5): This compound was prepared from *tert*-butyl (*R*)-3-aminopiperidine-1-carboxylate as described in the synthesis of **8** as a light-yellow solid (95%). 1H NMR (300 MHz, DMSO- d_6) δ 9.94 (s, 1H), 8.66 (s, 2H), 8.27 (s, 1H), 8.09 (s, 1H), 7.97 (d, $J = 9.8$ Hz, 1H), 7.57 (d, $J = 6.8$ Hz, 1H), 7.36–6.82 (m, 2H), 4.15 (s, 1H), 4.01–3.77 (m, 3H), 3.31–2.87 (m, 4H), 2.13–1.85 (m, 2H), 1.84–1.57 (m, 2H). ^{13}C NMR (126 MHz, DMSO- d_6) δ 155.86, 153.28, 138.11, 136.28, 135.40 (t, $J = 27.4$ Hz), 126.64, 126.37, 121.63, 117.09, 115.20, 112.20 (t, $J = 231.6$ Hz), 44.99, 43.88, 43.02, 26.91, 18.99. ESI-HRMS m/z $[M+H]^+$ calcd for $C_{17}H_{21}F_2N_8O$: 391.1801, found: 391.1797.

(*R*)-*N*-(3-(difluoromethyl)-1-methyl-1*H*-pyrazol-4-yl)-2-methyl-5-(piperidin-3-ylamino)pyrazolo

[1,5- α]pyrimidine-3-carboxamide trifluoroacetate (4-Me): A solution of ethyl 5-chloro-2-methylpyrazolo[1,5- α]pyrimidine-3-carboxylate **44** (CAS NO. 1431654-56-6, 50 mg, 0.209 mmol), *tert*-butyl (*R*)-3-aminopiperidine-1-carboxylate (84 mg, 0.417 mmol) and potassium fluoride (121 mg, 2.09 mmol) was stirred at 100 °C for 2 h. The mixture was allowed to cool to room temperature and the reaction was taken up in ethyl acetate (15 mL), and the organics were washed with water and brine. The organic phase was dried over anhydrous sodium sulfate, filtered, and concentrated. The residue was purified by prep-TLC (5% MeOH in DCM) to afford ethyl (*R*)-5-((1-(*tert*-butoxycarbonyl)piperidin-3-yl)amino)-2-methylpyrazolo[1,5- α]pyrimidine-3-carboxylate as pale-yellow solid (83 mg, 99%). MS (ESI): 404.3 $[M+H]^+$. Then the solid (50 mg, 0.124 mmol) dissolved in methanol/tetrahydrofuran/water (1 mL/1 mL/0.3 mL), followed by addition of lithium hydroxide monohydrate (31 mg, 0.744 mmol) was stirred at 50 °C overnight. The solvent was removed in vacuo. The residue was adjusted pH to 3-4 with 1 mol/L hydrochloric acid upon which precipitate formed. The precipitate was filtered off, washed with water and dried to afford intermediate **45** as a white solid (36 mg, 75%). 1H NMR (400 MHz, Chloroform- d) δ 10.59 (brs, 1H), 8.17 (s, 1H), 6.16 (s, 1H), 5.76 (brs, 1H), 4.13 (s, 1H) 3.88–3.13 (m, 4H), 2.62 (s, 3H), 2.10–1.82 (m, 2H), 1.81–1.67 (m, 2H). MS (ESI): 374.1 $[M-H]^-$.

Compound **4-Me** was prepared from intermediates **45** and **25** by the similar procedure of synthesis of **2** as a light-yellow solid (64%). ^1H NMR (400 MHz, DMSO- d_6) δ 9.40 (s, 1H), 8.57 (d, J = 7.3 Hz, 3H), 8.30 (s, 1H), 8.04 (s, 1H), 7.10 (t, J = 54.2 Hz, 1H), 6.41 (d, J = 7.6 Hz, 1H), 4.48–4.29 (m, 1H), 3.87 (s, 3H), 3.32–2.94 (m, 4H), 2.13–1.89 (m, 2H), 1.82–1.55 (m, 2H). ^{13}C NMR (151 MHz, DMSO- d_6) δ 160.23, 156.27, 154.95, 146.74, 135.75, 134.04 (t, J = 29.1 Hz), 125.19, 118.44, 118.03, 116.04, 112.79 (t, J = 229.7 Hz), 100.91, 97.46, 45.43, 43.11, 42.97, 26.98, 18.91, 14.64. ESI-HRMS m/z $[M+H]^+$ calcd for $\text{C}_{18}\text{H}_{23}\text{F}_2\text{N}_8\text{O}_2$: 405.1957, found: 415.1966.

(R)-N-(3-(difluoromethyl)-1-methyl-1H-pyrazol-4-yl)-2-methyl-6-(piperidin-3-ylamino)imidazo[1,2-b]pyridazine-3-carboxamide trifluoroacetate (5-Me): Intermediate **47** was prepared from intermediate **25** and ethyl 6-chloro-2-methylimidazo[1,2-*b*]pyridazine-3-carboxylate **46** (CAS NO.14714-18-2) by the similar procedure of synthesis of **37** as white solid (56%). ^1H NMR (400 MHz, Chloroform-*d*) δ 10.79 (s, 1H), 8.36 (s, 1H), 7.98 (d, J = 9.4 Hz, 1H), 6.83 (t, J = 54.5 Hz, 1H), 3.92 (t, J = 1.2 Hz, 3H), 2.89 (s, 3H). MS (ESI): 341.1 $[M+H]^+$.

Compound **5-Me** was prepared from intermediate **47** and *tert*-butyl (*R*)-3-aminopiperidine-1-carboxylate by the similar procedure of synthesis of **8** as a white solid (71%). ^1H NMR (400 MHz, DMSO- d_6) δ 10.08 (s, 1H), 8.55 (s, 2H), 8.30 (s, 1H), 7.88 (d, J = 9.7 Hz, 1H), 7.45 (d, J = 6.7 Hz, 1H), 7.12 (t, J = 54.3 Hz, 1H), 6.90 (d, J = 9.7 Hz, 1H), 4.20–4.05 (m, 1H), 3.90 (s, 3H), 3.24–2.92 (m, 4H), 2.58 (s, 3H), 2.07–1.86 (m, 2H), 1.76–1.56 (m, 2H). ^{13}C NMR (151 MHz, DMSO- d_6) δ 156.84, 152.94, 146.59, 135.76, 135.37 (t, J = 27.2 Hz), 126.44, 125.68, 117.18, 116.99, 115.11, 112.29 (t, J = 231.3 Hz), 45.00, 43.94, 43.02, 26.99, 19.04, 15.79. ESI-HRMS m/z $[M+H]^+$ calcd for $\text{C}_{18}\text{H}_{23}\text{F}_2\text{N}_8\text{O}_2$: 405.1957, found: 415.1961.

(S)-N-(3-(difluoromethyl)-1-methyl-1H-pyrazol-4-yl)-6-(piperidin-3-ylamino)imidazo[1,2-b]pyridazine-3-carboxamide trifluoroacetate (6): This compound was prepared from *tert*-butyl (3*S*)-3-aminocyclohexane-1-carboxylate as described in the synthesis of **8** as a white solid (56%). ^1H NMR (400 MHz, DMSO- d_6) δ 9.94 (s, 1H), 8.62 (s, 2H), 8.27 (s, 1H), 8.08 (s, 1H), 7.97 (d, J = 9.7 Hz, 1H), 7.56 (d, J = 6.8 Hz, 1H), 7.13 (t, J = 54.2 Hz, 1H), 6.93 (d, J = 9.8 Hz, 1H), 4.15 (s, 1H), 3.91 (s, 3H), 3.20 (s, 2H), 3.07 (m, 2H), 1.99 (d, J = 9.9 Hz, 2H), 1.69 (s, 2H). ^{13}C NMR (126 MHz, DMSO- d_6) δ 155.84, 153.32, 138.05, 136.13, 135.41 (t, J = 27.5 Hz), 126.57, 126.37, 121.65,

117.67, 117.09, 115.30, 112.21 (t, $J = 231.2$ Hz), 45.02, 43.89, 43.02, 26.91, 18.99. ESI-HRMS m/z $[M+H]^+$ calcd for $C_{17}H_{21}F_2N_8O$: 391.1801, found: 391.1791.

(R)-N-(3-(difluoromethyl)-1-methyl-1H-pyrazol-4-yl)-6-(pyrrolidin-3-ylamino)imidazo[1,2-b]

pyridazine-3-carboxamide trifluoroacetate (7): This compound was prepared from *tert*-butyl (*R*)-3-aminopyrrolidine-1-carboxylate as described in the synthesis of **8** as a white solid (61%). 1H NMR (400 MHz, DMSO- d_6) δ 9.94 (s, 1H), 8.62 (s, 2H), 8.27 (s, 1H), 8.08 (s, 1H), 7.97 (d, $J = 9.7$ Hz, 1H), 7.56 (d, $J = 6.8$ Hz, 1H), 7.13 (t, $J = 54.2$ Hz, 1H), 6.93 (d, $J = 9.8$ Hz, 1H), 4.15 (s, 1H), 3.91 (s, 3H), 3.20 (s, 2H), 3.14–2.95 (m, 2H), 1.99 (d, $J = 9.9$ Hz, 2H), 1.69 (s, 2H). ^{13}C NMR (126 MHz, DMSO- d_6) δ 156.49, 153.72, 138.72, 137.06, 135.14 (t, $J = 27.8$ Hz), 127.36, 126.77, 121.98, 118.84, 117.60, 115.36, 112.73 (t, $J = 230.9$ Hz), 50.20, 49.66, 44.49, 30.24. ESI-HRMS m/z $[M+H]^+$ calcd for $C_{16}H_{19}F_2N_8O$: 377.1644, found: 377.1651.

(R)-6-(3-aminopyrrolidin-1-yl)-N-(3-(difluoromethyl)-1-methyl-1H-pyrazol-4-yl)imidazo[1,2-b]

pyridazine-3-carboxamide trifluoroacetate (8): A mixture of *N,N*-dimethylformamide dimethyl acetal (8.40 g, 70.5 mmol) and 6-chloropyridazin-3-amine **34** (8.70 g, 67.2 mmol) was stirred at 110 °C for 2 h. After cooling, The off-white solid precipitated was collected by filtration and washed with ethyl acetate (20 mL) and dried to afford (*E*)-*N'*-(6-chloropyridazin-3-yl)-*N,N*-dimethylformimidamide **35** (8.90 g, 72%). 1H NMR (300 MHz, DMSO- d_6) δ 8.47 (s, 1H), 7.57 (d, $J = 9.1$ Hz, 1H), 7.14 (d, $J = 9.1$ Hz, 1H), 3.12 (s, 3H), 3.01 (s, 3H).

A mixture of compound **35** (2.35 g, 12.7 mmol) and ethyl bromoacetate (3.88 mL, 38.2 mmol) in acetonitrile (20 mL) was stirred at 80 °C for 3 h. After cooling to room temperature, a large amount of solids precipitated, which was filtered off with suction, washed with diethyl ether (20 mL), recrystallized with ethyl acetate/acetonitrile (2:5, 35 mL) to afford yellow crystalline solid (1.8 g). The solid was dissolved in a solution of *N,N*-diisopropylethylamine (1.69 mL, 10.2 mmol) in acetonitrile (25 mL). The reaction mixture was stirred for 3 h at room temperature. The solvent was removed in vacuo and the residue was triturated with water to afford ethyl 6-chloroimidazo[1,2-*b*]pyridazine-3-carboxylate **36** as a light brown solid (960 mg, 83%). 1H NMR

(300 MHz, DMSO- d_6) δ 8.46–8.31 (m, 2H), 7.63 (d, J = 9.5 Hz, 1H), 4.36 (q, J = 7.1 Hz, 2H), 1.34 (t, J = 7.1 Hz, 3H).

A mixture of compound **36** (600 mg, 2.66 mmol) and Lithium hydroxide monohydrate (335 mg, 7.98 mmol) in tetrahydrofuran/water (10 mL/2.5 mL) was stirred at 35 °C for 4 h. The solvent was removed in vacuo. The residue was added water (4 mL) and adjusted pH to 3-4 with 1 mol/L hydrochloric acid upon which precipitate formed. The precipitate was filtered off, washed with water and dried to afford 6-chloroimidazo[1,2-*b*]pyridazine-3-carboxylic acid **37** as an off-white solid (519 mg, 98%). ^1H NMR (400 MHz, DMSO- d_6) δ 13.30 (s, 1H), 8.63–8.20 (m, 2H), 7.61 (d, J = 9.5 Hz, 1H).

A solution of compound **37** (300 mg, 1.52 mmol), 3-(difluoromethyl)-1-methyl-1*H*-pyrazol-4-amine **25** (203 mg, 1.38 mmol), EDCI (317 mg, 1.66 mmol), HOBT (223 mg, 1.66 mmol) and *N,N*-diisopropylethylamine (570 μL , 3.45 mmol) in DMF (10 mL) was stirred overnight at room temperature. The reaction was taken up in ethyl acetate (50 mL), and the organics were washed with water and brine. The organic phase was dried over anhydrous sodium sulfate, filtered, and concentrated. The residue was purified by flash column chromatography eluting with 1% MeOH in DCM to afford compound **38** as a white solid (303 mg, 67%). ^1H NMR (300 MHz, DMSO- d_6) δ 8.47 (s, 1H), 7.57 (d, J = 9.1 Hz, 1H), 7.14 (d, J = 9.1 Hz, 1H), 3.12 (s, 3H), 3.01 (s, 3H). MS (ESI): 349.2 [$M+\text{Na}$] $^+$.

A mixture of intermediate **38** (40 mg, 0.122 mmol), *tert*-butyl (*R*)-pyrrolidin-3-ylcarbamate (46 mg, 0.244 mmol), potassium fluoride (71 mg, 1.22 mmol), and *N,N*-diisopropylethylamine (61 μL , 0.367 mmol) in DMSO (2 mL) was stirred at 100 °C for 45 minutes. The reaction was taken up in ethyl acetate (15 mL), and the organics were washed with water and brine. The organic phase was dried over anhydrous sodium sulfate, filtered, and concentrated. The residue was purified by prep-TLC (6% MeOH in DCM) to afford *tert*-butyl (*R*)-(1-(3-((3-(difluoromethyl)-1-methyl-1*H*-pyrazol-4-yl)carbamoyl)imidazo[1,2-*b*]pyridazin-6-yl)pyrrolidin-3-yl)carbamate as a colorless liquid (76 mg, 90%). ^1H NMR (400 MHz, Chloroform-*d*) δ 10.23 (s, 1H), 8.39 (s, 1H), 8.30 (s, 1H), 7.80 (d, J = 9.8 Hz, 1H), 6.92 – 6.57 (m, 2H), 4.85 (s, 1H), 4.42 (s, 1H), 3.92 (d, J = 1.3 Hz, 3H), 3.85

(dd, $J = 10.8, 6.1$ Hz, 1H), 3.69 (dq, $J = 14.4, 7.2$ Hz, 2H), 3.44 (dd, $J = 10.9, 4.5$ Hz, 1H), 2.36 (dq, $J = 13.5, 7.0$ Hz, 1H), 2.12 – 2.00 (m, 1H), 1.46 (s, 9H).

A solution of *tert*-butyl (*R*)-(1-(3-((3-(difluoromethyl)-1-methyl-1*H*-pyrazol-4-yl)carbamoyl)imidazo[1,2-*b*]pyridazin-6-yl)pyrrolidin-3-yl)carbamate (76 mg, 0.159 mmol) in dichloromethane (4 mL) was added trifluoroacetic acid (1 mL). The mixture was stirred at room temperature for 2 h. The solvent was removed under reduced pressure and the residue was purified by triturating with methanol/diethyl ether (1 mL/5 mL) to afford compound **8** as a white solid (77 mg, 98%). ^1H NMR (400 MHz, DMSO- d_6) δ 10.15 (s, 1H), 8.39 (s, 1H), 8.19 (s, 3H), 8.17 (s, 1H), 8.09 (d, $J = 9.9$ Hz, 1H), 7.30–6.96 (m, 2H), 4.04 (s, 1H), 3.91 (s, 3H), 3.81 (dd, $J = 11.9, 5.9$ Hz, 1H), 3.77–3.56 (m, 3H), 2.38 (dq, $J = 14.7, 8.0$ Hz, 1H), 2.14 (dd, $J = 13.1, 5.8$ Hz, 1H). ^{13}C NMR (126 MHz, DMSO- d_6) δ 155.50, 152.72, 137.74, 136.61, 134.60 (t, $J = 28.2$ Hz), 126.69, 125.95, 121.22, 117.15, 114.95, 112.84, 112.30 (t, $J = 230.3$ Hz), 50.80, 49.51, 44.86, 28.96. ESI-HRMS m/z [$M+H$] $^+$ calcd for $\text{C}_{16}\text{H}_{19}\text{F}_2\text{N}_8\text{O}$: 377.1644, found: 377.1645.

(*R*)-6-(azepan-3-ylamino)-*N*-(3-(difluoromethyl)-1-methyl-1*H*-pyrazol-4-yl)imidazo[1,2-*b*]

pyridazine-3-carboxamide trifluoroacetate (9): This compound was prepared from *tert*-butyl (*R*)-3-aminoazepane-1-carboxylate as described in the synthesis of **8** as a light-yellow solid (65%). ^1H NMR (400 MHz, DMSO- d_6) δ 9.97 (s, 1H), 8.79 (d, $J = 58.3$ Hz, 2H), 8.27 (s, 1H), 8.11 (s, 1H), 7.97 (d, $J = 9.8$ Hz, 1H), 7.57 (d, $J = 6.9$ Hz, 1H), 7.14 (t, $J = 54.1$ Hz, 1H), 6.95 (d, $J = 9.7$ Hz, 1H), 4.30 (s, 1H), 3.91 (s, 3H), 3.48–3.39 (m, 1H), 3.34–3.18 (m, 2H), 3.07 (s, 1H), 2.12–1.96 (m, 1H), 1.96–1.68 (m, 4H), 1.69–1.50 (m, 1H). ^{13}C NMR (126 MHz, DMSO- d_6) δ 155.99, 153.10, 138.15, 136.21, 135.32 (t, $J = 26.9$ Hz), 126.61, 126.25, 121.47, 117.75, 117.16, 115.34, 112.10 (t, $J = 231.3$ Hz), 47.99, 47.52, 46.98, 31.29, 25.39, 21.77. ESI-HRMS m/z [$M+H$] $^+$ calcd for $\text{C}_{18}\text{H}_{23}\text{F}_2\text{N}_8\text{O}$: 405.1957, found: 405.1949.

6-(4-aminopiperidin-1-yl)-*N*-(3-(difluoromethyl)-1-methyl-1*H*-pyrazol-4-yl)imidazo[1,2-*b*]

pyridazine-3-carboxamide trifluoroacetate (10): This compound was prepared from *tert*-butyl piperidin-4-ylcarbamate as described in the synthesis of **8** as a white solid (88%). ^1H NMR (400 MHz, DMSO- d_6) δ 9.96 (s, 1H), 8.41 (s, 1H), 8.16 (s, 1H), 7.99 (d, $J = 4.7$ Hz, 3H), 7.47 (d, $J = 10.1$ Hz, 1H), 7.17 (t, $J = 53.8$ Hz, 1H), 4.29 (d, $J = 13.3$ Hz, 2H), 3.91 (s, 3H), 3.39–3.30 (m, 1H),

3.17–2.98 (m, 2H), 2.02 (d, $J = 12.5$ Hz, 2H), 1.60 (qd, $J = 12.8, 4.4$ Hz, 2H). ^{13}C NMR (126 MHz, DMSO- d_6) δ 155.42, 154.97, 138.05, 137.72, 134.19 (t, $J = 28.5$ Hz), 127.12, 125.78, 121.47, 117.25, 112.76, 112.43 (t, $J = 230.1$ Hz), 47.27, 43.94, 28.92. ESI-HRMS m/z $[M+H]^+$ calcd for $\text{C}_{17}\text{H}_{21}\text{F}_2\text{N}_8\text{O}$: 391.1801, found: 391.1798.

6-((2-aminoethyl)amino)-*N*-(3-(difluoromethyl)-1-methyl-1*H*-pyrazol-4-yl)imidazo[1,2-*b*]

pyridazine-3-carboxamide trifluoroacetate (11): This compound was prepared from *tert*-butyl (2-aminoethyl)carbamate as described in the synthesis of **8** as a white solid (95%). ^1H NMR (400 MHz, DMSO- d_6) δ 10.09 (s, 1H), 8.35 (s, 1H), 8.12 (s, 1H), 7.97 (d, $J = 9.8$ Hz, 1H), 7.74 (s, 1H), 7.14 (t, $J = 53.9$ Hz, 1H), 6.91 (d, $J = 9.8$ Hz, 1H), 3.90 (s, 3H), 3.58 (q, $J = 5.6$ Hz, 2H), 3.09 (q, $J = 5.7$ Hz, 2H). ^{13}C NMR (126 MHz, DMSO- d_6) δ 155.59, 154.13, 137.98, 135.94, 126.27, 125.86, 121.52, 117.27, 115.59, 115.00, 112.33 (t, $J = 230.5$ Hz), 38.59, 37.52. ESI-HRMS m/z $[M+H]^+$ calcd for $\text{C}_{14}\text{H}_{17}\text{F}_2\text{N}_8\text{O}$: 351.1492, found: 351.1488.

***N*-(3-(difluoromethyl)-1-methyl-1*H*-pyrazol-4-yl)-6-(piperazin-1-yl)imidazo[1,2-*b*]pyridazine-3-carboxamide trifluoroacetate (12):**

This compound was prepared from *tert*-butyl piperazine-1-carboxylate as described in the synthesis of **8** as a white solid (89%). ^1H NMR (400 MHz, DMSO- d_6) δ 9.89 (s, 1H), 9.06 (s, 2H), 8.40 (s, 1H), 8.19 (s, 1H), 8.17 (d, $J = 10.0$ Hz, 1H), 7.47 (d, $J = 10.1$ Hz, 1H), 7.17 (t, $J = 53.8$ Hz, 1H), 3.91 (s, 3H), 3.81 (t, $J = 5.2$ Hz, 4H), 3.28 (t, $J = 5.2$ Hz, 4H). ^{13}C NMR (126 MHz, DMSO- d_6) δ 155.30, 154.80, 138.28, 137.93, 134.18 (t, $J = 28.2$ Hz), 127.35, 125.71, 121.56, 117.28, 112.61, 112.52 (t, $J = 230.1$ Hz), 42.63, 42.19. ESI-HRMS m/z $[M+H]^+$ calcd for $\text{C}_{16}\text{H}_{19}\text{F}_2\text{N}_8\text{O}$: 377.1644, found: 377.1638.

(*R*)-*N*-(3-(difluoromethyl)-1-methyl-1*H*-pyrazol-4-yl)-6-(methyl(piperidin-3-yl)amino)imidazo

[1,2-*b*]pyridazine-3-carboxamide trifluoroacetate (13): This compound was prepared from *tert*-butyl (*R*)-3-(methylamino)piperidine-1-carboxylate as described in the synthesis of **8** as a white solid (35%). ^1H NMR (400 MHz, Methanol- d_4) δ 8.28 (s, 1H), 8.18 (s, 1H), 7.93 (s, 1H), 7.37 (s, 1H), 6.88 (t, $J = 54.2$ Hz, 1H), 4.36 (d, $J = 12.0$ Hz, 1H), 3.93 (s, 3H), 3.42 (s, 2H), 3.13 (s, 3H), 3.00 (s, 1H), 2.00 (d, $J = 65.1$ Hz, 4H). ^{13}C NMR (126 MHz, Methanol- d_4) δ 158.18, 156.47, 139.76, 138.3, 137.08 (t, $J = 28.1$ Hz), 127.77, 127.50, 123.16, 118.40, 113.76 (t, $J = 230.9$ Hz), 113.60, 53.55,

46.17, 44.56, 39.76, 31.29, 27.44, 23.05. ESI-HRMS m/z $[M+H]^+$ calcd for $C_{18}H_{23}F_2N_8O$: 405.1957, found: 405.1961.

(R)-N-(1-methyl-3-(trifluoromethyl)-1H-pyrazol-4-yl)-6-(piperidin-3-ylamino)imidazo[1,2-b]

pyridazine-3-carboxamide trifluoroacetate (14): A mixture of ethyl 6-chloroimidazo[1,2-*b*]pyridazine-3-carboxylate **36** (600 mg, 2.66 mmol), *tert*-butyl (*R*)-3-aminopiperidine-1-carboxylate (960 mg, 4.79 mmol) and potassium fluoride (1.54 g, 26.6 mmol) in DMSO (8 mL) was stirred overnight at 100°C. The reaction was taken up in ethyl acetate (50 mL), and the organics were washed with water and brine. The organic phase was dried over anhydrous sodium sulfate, filtered, and concentrated. The residue was purified by flash column chromatography eluting with 1% to 2% MeOH in DCM to afford intermediate ethyl (*R*)-6-((1-(*tert*-butoxycarbonyl)piperidin-3-yl)amino)imidazo[1,2-*b*]pyridazine-3-carboxylate (620 mg, 60%) as a light yellow oil. 1H NMR (300 MHz, DMSO- d_6) δ 8.00 (s, 1H), 7.84 (d, J = 9.7 Hz, 1H), 7.08 (d, J = 6.1 Hz, 1H), 6.90 (d, J = 9.7 Hz, 1H), 4.29 (q, J = 7.1 Hz, 2H), 4.02–3.65 (m, 2H), 1.97 (s, 1H), 1.79 (s, 1H), 1.61 (s, 1H), 1.38 (s, 3H), 1.35–1.25 (m, 4H), 1.12 (s, 6H).

A mixture of ethyl (*R*)-6-((1-(*tert*-butoxycarbonyl)piperidin-3-yl)amino)imidazo[1,2-*b*]pyridazine-3-carboxylate (620 mg, 1.59 mmol) and lithium hydroxide monohydrate (200 mg, 4.78 mmol) in methanol/tetrahydrofuran/water (9 mL/9 mL/3 mL) was stirred at 35 °C for 4 h. The solvent was removed in vacuo. The residue was added water (4 mL) and adjusted pH to 3-4 with 1 mol/L hydrochloric acid upon which precipitate formed. The precipitate was filtered off, washed with water and dried to afford (*R*)-6-((1-(*tert*-butoxycarbonyl)piperidin-3-yl)amino)imidazo[1,2-*b*]pyridazine-3-carboxylic acid **39** as an off-white solid (320 mg, 56%). 1H NMR (300 MHz, DMSO- d_6) δ 12.48 (s, 1H), 7.97 (s, 1H), 7.85 (d, J = 9.7 Hz, 1H), 7.14 (d, J = 6.1 Hz, 1H), 6.90 (d, J = 9.7 Hz, 1H), 3.72 (s, 2H), 3.38 (s, 2H), 3.29–3.10 (m, 1H), 2.06–1.88 (m, 1H), 1.79 (s, 1H), 1.61 (s, 1H), 1.50–1.32 (m, 3H), 1.13 (s, 7H). MS (ESI): 360.3 $[M-H]^-$.

A solution of intermediate **39** (70 mg, 0.193 mmol), 1-methyl-3-(trifluoromethyl)-1H-pyrazol-4-amine **33a** (35 mg, 0.213 mmol), EDCI (45 mg, 0.232 mmol), HOBT (32 mg, 0.232 mmol) and *N,N*-diisopropylethylamine (80 μ L, 0.484 mmol) in DMF (2 mL) was stirred overnight at room temperature. The reaction was taken up in ethyl acetate, washed with water and brine. The

organic phase was dried over anhydrous sodium sulfate, filtered, and concentrated. The residue was purified by prep-TLC (6% MeOH in DCM) to afford *tert*-butyl (*R*)-3-((3-((1-methyl-3-(trifluoromethyl)-1*H*-pyrazol-4-yl)carbamoyl)imidazo[1,2-*b*]pyridazin-6-yl)amino)piperidine-1-carboxylate (60 mg, 61%). Then it dissolved in dichloromethane (4 mL) which was added trifluoroacetic acid (1 mL). The mixture was stirred at room temperature for 2 h. The solvent was removed under reduced pressure and the residue was purified by triturating with methanol/diethyl ether (1 mL/5 mL) to afford compound **14** as a white solid (40 mg, 78%). ¹H NMR (400 MHz, DMSO-*d*₆) δ 9.87 (s, 1H), 8.67 (s, 2H), 8.32 (s, 1H), 8.09 (s, 1H), 7.98 (d, *J* = 9.8 Hz, 1H), 7.59 (d, *J* = 7.1 Hz, 1H), 6.92 (d, *J* = 9.8 Hz, 1H), 4.07 (s, 1H), 3.96 (s, 3H), 3.23 (d, *J* = 11.8 Hz, 1H), 3.11 (d, *J* = 19.2 Hz, 2H), 2.99 (s, 1H), 2.09–1.88 (m, 2H), 1.66 (d, *J* = 7.0 Hz, 2H). ¹³C NMR (126 MHz, DMSO-*d*₆) δ 156.40, 153.30, 138.19, 136.33, 131.79 (q, *J* = 35.8 Hz), 128.17, 126.72, 121.52 (q, *J* = 268.2 Hz), 121.47, 117.02, 115.21, 45.23, 44.17, 42.89, 27.14, 19.29. ESI-HRMS *m/z* [*M*+*H*]⁺ calcd for C₁₇H₂₀F₃N₈O: 409.1707, found: 407.1719.

(*R*)-*N*-(3-cyano-1-methyl-1*H*-pyrazol-4-yl)-6-(piperidin-3-ylamino)imidazo[1,2-*b*]pyridazine-3-carboxamide trifluoroacetate (15): This compound was prepared from intermediate **29** as described in the synthesis of **14** as an off-white solid (69%). ¹H NMR (300 MHz, DMSO-*d*₆) δ 10.30 (s, 1H), 8.66 (s, 2H), 8.41 (s, 1H), 8.12 (s, 1H), 7.99 (d, *J* = 9.8 Hz, 1H), 7.65 (d, *J* = 6.8 Hz, 1H), 6.95 (d, *J* = 9.8 Hz, 1H), 4.27 (s, 1H), 3.98 (s, 3H), 3.36–3.24 (m, 1H), 3.24–2.97 (m, 3H), 1.99 (d, *J* = 11.8 Hz, 2H), 1.74 (d, *J* = 9.2 Hz, 2H). ¹³C NMR (126 MHz, DMSO-*d*₆) δ 155.74, 153.17, 138.31, 136.66, 126.77, 125.24, 124.58, 121.20, 115.18, 113.56, 45.06, 44.25, 43.07, 26.81, 19.15. ESI-HRMS *m/z* [*M*+*H*]⁺ calcd for C₁₇H₂₀N₉O: 366.1785, found: 366.1795.

(*R*)-*N*-(3-carbamoyl-1-methyl-1*H*-pyrazol-4-yl)-6-(piperidin-3-ylamino)imidazo[1,2-*b*]pyridazine-3-carboxamide trifluoroacetate (16): This compound was prepared from intermediate **27** as described in the synthesis of **14** as an off-white solid (quant). ¹H NMR (300 MHz, DMSO-*d*₆) δ 10.68 (s, 1H), 8.88 (s, 1H), 8.53 (s, 1H), 8.36 (s, 1H), 8.17 (d, *J* = 10.6 Hz, 2H), 7.94 (d, *J* = 10.2 Hz, 2H), 7.56 (s, 1H), 6.91 (d, *J* = 9.7 Hz, 1H), 4.63 (s, 1H), 3.95 (s, 3H), 3.46 (d, *J* = 11.8 Hz, 2H), 2.82 (dd, *J* = 47.4, 10.9 Hz, 2H), 1.97 (d, *J* = 22.2 Hz, 2H), 1.80–1.52 (m, 2H). ¹³C NMR (126 MHz, DMSO-*d*₆) δ 165.79, 155.22, 153.64, 138.03, 136.83, 131.97, 126.28, 124.92, 122.06, 122.00,

115.31, 46.43, 43.63, 43.06, 28.10, 20.97. ESI-HRMS m/z $[M+H]^+$ calcd for $C_{17}H_{22}N_9O_2$: 384.1891, found: 384.1901.

(R)-N-(1,3-dimethyl-1H-pyrazol-4-yl)-6-(piperidin-3-ylamino)imidazo[1,2-b]pyridazine-3-

carboxamide trifluoroacetate (17): This compound was prepared from 1,3-dimethyl-1H-pyrazol-4-amine as described in the synthesis of **14** as a white solid (95%). 1H NMR (400 MHz, Methanol- d_4) δ 8.18 (s, 1H), 7.90 (d, J = 10.1 Hz, 2H), 7.04 (d, J = 9.8 Hz, 1H), 4.23 (d, J = 7.0 Hz, 1H), 3.85 (s, 3H), 3.49 (dd, J = 12.0, 3.2 Hz, 1H), 3.25 (d, J = 7.4 Hz, 1H), 3.15 (d, J = 12.2 Hz, 1H), 2.27 (s, 3H), 2.24–2.18 (m, 1H), 2.18–2.06 (m, 1H), 1.90–1.76 (m, 2H). ^{13}C NMR (126 MHz, DMSO- d_6) δ 155.77, 153.14, 139.33, 137.63, 135.21, 126.43, 124.98, 122.19, 116.98, 114.92, 45.26, 44.52, 42.95, 38.47, 27.08, 19.43, 11.23. ESI-HRMS m/z $[M+H]^+$ calcd for $C_{17}H_{23}N_8O$: 355.1989, found: 355.1998.

(R)-N-(1-ethyl-3-(trifluoromethyl)-1H-pyrazol-4-yl)-6-(piperidin-3-ylamino)imidazo[1,2-b]

pyridazine-3-carboxamide trifluoroacetate (18): This compound was prepared from intermediate **33b** as described in the synthesis of **14** as a light-yellow solid (66%). 1H NMR (400 MHz, DMSO- d_6) δ 9.87 (s, 1H), 8.67 (s, 2H), 8.38 (s, 1H), 8.08 (s, 1H), 7.98 (d, J = 9.7 Hz, 1H), 7.58 (d, J = 7.2 Hz, 1H), 6.92 (d, J = 9.8 Hz, 1H), 4.25 (q, J = 7.3 Hz, 2H), 4.08 (s, 1H), 3.22 (s, 1H), 3.14 (s, 1H), 3.08 (s, 1H), 2.99 (s, 1H), 2.10–1.86 (m, 2H), 1.66 (s, 2H), 1.42 (t, J = 7.3 Hz, 3H). ^{13}C NMR (126 MHz, DMSO- d_6) δ 156.37, 153.30, 138.22, 136.42, 131.63 (q, J = 35.5 Hz), 126.76, 121.5 (q, J = 267.8 Hz), 121.45, 117.81, 116.92, 115.45, 115.14, 47.50, 45.27, 44.15, 42.88, 27.20, 19.32, 15.07. ESI-HRMS m/z $[M+H]^+$ calcd for $C_{18}H_{22}F_3N_8O$: 423.1863, found: 423.1869.

(R)-N-(1-isopropyl-3-(trifluoromethyl)-1H-pyrazol-4-yl)-6-(piperidin-3-ylamino)imidazo[1,2-b]

pyridazine-3-carboxamide trifluoroacetate (19): This compound was prepared from intermediate **33c** as described in the synthesis of **14** as a light-yellow solid (39%). 1H NMR (400 MHz, DMSO- d_6) δ 9.87 (s, 1H), 8.68 (s, 2H), 8.39 (s, 1H), 8.08 (s, 1H), 7.98 (d, J = 9.8 Hz, 1H), 7.58 (d, J = 7.2 Hz, 1H), 6.92 (d, J = 9.8 Hz, 1H), 4.64 (h, J = 6.7 Hz, 1H), 4.09 (s, 1H), 3.24 (d, J = 11.8 Hz, 1H), 3.15 (s, 1H), 3.06 (s, 1H), 2.99 (s, 1H), 2.09–1.87 (m, 2H), 1.64 (d, J = 9.7 Hz, 2H), 1.46 (d, J = 6.6 Hz, 6H). ^{13}C NMR (126 MHz, DMSO- d_6) δ 156.36, 153.31, 138.25, 136.45, 131.33 (q, J = 35.7

Hz), 126.78, 125.19, 121.60 (q, $J = 268.9$ Hz), 121.46, 116.81, 115.53, 115.11, 54.51, 45.32, 44.15, 42.87, 27.23, 22.33, 19.35. ESI-HRMS m/z $[M+H]^+$ calcd for $C_{19}H_{24}F_3N_8O$: 437.2020, found: 437.2032.

(R)-6-(piperidin-3-ylamino)-N-(1-(piperidin-4-yl)-3-(trifluoromethyl)-1H-pyrazol-4-yl)imidazo

[1,2-*b*]pyridazine-3-carboxamide trifluoroacetate (20): This compound was prepared from intermediate **33d** as described in the synthesis of **14** as a light-yellow solid (87%). 1H NMR (400 MHz, DMSO- d_6) δ 9.91 (s, 1H), 8.92 (d, $J = 11.3$ Hz, 1H), 8.79 (s, 2H), 8.59 (d, $J = 11.1$ Hz, 1H), 8.43 (s, 1H), 8.11 (s, 1H), 7.99 (d, $J = 9.7$ Hz, 1H), 7.63 (d, $J = 7.3$ Hz, 1H), 6.94 (d, $J = 9.6$ Hz, 1H), 4.67 (td, $J = 10.8, 10.4, 5.5$ Hz, 1H), 4.11 (s, 1H), 3.45 (d, $J = 12.8$ Hz, 2H), 3.23 (d, $J = 12.1$ Hz, 1H), 3.19–2.89 (m, 5H), 2.24 (d, $J = 13.2$ Hz, 2H), 2.15 (t, $J = 12.4$ Hz, 2H), 1.99 (d, $J = 11.8$ Hz, 2H), 1.66 (s, 2H). ^{13}C NMR (126 MHz, DMSO- d_6) δ 156.37, 153.37, 136.43, 131.82 (q, $J = 35.9$ Hz), 126.75, 125.87, 121.49, 121.44 (q, $J = 268.7$ Hz), 117.14, 115.28, 56.27, 45.32, 44.08, 42.86, 42.23, 28.39, 27.21, 19.31. ESI-HRMS m/z $[M+H]^+$ calcd for $C_{21}H_{29}F_3N_9O$: 478.2285, found: 478.2282.

(R)-6-(piperidin-3-ylamino)-N-(1-(tetrahydro-2H-pyran-4-yl)-3-(trifluoromethyl)-1H-pyrazol-4-yl)

imidazo[1,2-*b*]pyridazine-3-carboxamide trifluoroacetate (21): This compound was prepared from intermediate **33e** as described in the synthesis of **14** as a light-yellow solid (68%). 1H NMR (400 MHz, DMSO- d_6) δ 9.88 (s, 1H), 8.71 (s, 2H), 8.42 (s, 1H), 8.09 (s, 1H), 7.98 (d, $J = 9.7$ Hz, 1H), 7.60 (s, 1H), 6.93 (d, $J = 9.8$ Hz, 1H), 4.56 (d, $J = 11.5$ Hz, 1H), 4.09 (s, 1H), 4.04–3.88 (m, 2H), 3.47 (t, $J = 11.4$ Hz, 2H), 3.24 (s, 1H), 3.15 (s, 1H), 3.02 (d, $J = 31.5$ Hz, 2H), 2.08–1.88 (m, 6H), 1.66 (s, 2H). ^{13}C NMR (126 MHz, DMSO- d_6) δ 156.38, 153.34, 138.17, 136.29, 131.58 (q, $J = 36.3$ Hz), 126.70, 125.59, 121.53 (q, $J = 268.2$ Hz), 121.46, 117.58 (d, $J = 4.3$ Hz), 116.92, 115.22, 65.75, 58.38, 45.33, 44.17, 42.87, 32.53, 27.25, 19.38. ESI-HRMS m/z $[M+H]^+$ calcd for $C_{21}H_{26}F_3N_8O_2$: 479.2125, found: 479.2128.

Biological studies

Kinase activity inhibition assay: IRAK4 recombinant human protein (PV3362) was obtained from Thermo Fisher scientific. Kinase activity was evaluated using Z'-LYTE™ kinase assay kit (PV3180,

Thermo Fisher scientific) and all procedure involved in the experiment were processed according to Manufacturers' protocols. Dose–response curves obtained in dose inhibition assays against IRAK4 and IC₅₀ value of tested compounds were generated with Prism software (GraphPad Software) using four-parameter fit.

Kinase profile assay: The inhibitory activity against 20 kinases of compounds **4** and **5** was evaluated using enzyme-linked-immunosorbent assay (ELISA), according to previously described protocols. [29] Kinase proteins used in this assay were purchased from BPS Bioscience.

Chemical agents and cell culture: The BTK inhibitor ibrutinib (S2680) was from Selleckchem (Munich, Germany). MYD88 mutated DLBCL cancer cell lines used in this study (OCI-LY10 and TMD8) were purchased from the Cobioer Cell Bank (Nanjing, China). B cell lymphoma cell lines HT and Ramos were procured from DSMZ (Braunschweig, Germany). Cancer Cells were cultured in RPMI1640 medium supplemented with 10 % fetal bovine serum containing penicillin–streptomycin antibiotic solution, while plus 0.05 mM 2-mercaptoethanol for TMD8 cells, and incubated at 37 °C in a humidified incubator with a 5 % CO₂ atmosphere.

In vitro cytotoxicity assays: Cell killing ability of compounds against DLBCLs was assessed using CCK-8 assay. In brief, cells were seeded at densities of 10000-12000 cells per well in 96-well cell culture plates. Cells were then incubated with varying concentrations of each compound for 72h and cell viability was then evaluated by CCK-8 assay. The results were expressed as the mean 50% inhibitory concentration (IC₅₀), determined by the four-parameter Logit method.

Effect of the combination of the IRAK4 inhibitor and ibrutinib against DLBCL cells were also assessed by CCK-8 assay. The combination index (CI) values were calculated using the CalcuSyn software (Biosoft v2.0). CI value less than 1 is considered as synergistic effect, while greater than 1 is considered as an antagonistic effect.

Western blot: Approximately 2×10^6 cells were seeded into a 12-well plate and treated with compounds for 2 h. The cells were lysed with cell lysis buffer after washing with PBS twice. Cell lysates were collected for Western blot analysis and then blotted with primary antibodies against

phospho-IRAK4 (#11927), IRAK4 (#6956), phospho-IKK β (#2697), phospho-p65 (#3033) and β -actin (#3700). All antibodies were purchased from Cell Signaling Technology. The quantitative analysis of key proteins were conducted by Image J software.

Docking studies: The docking studies were carried out on Maestro 10.6 using the crystal structure (PDB code: 4Y73) obtained from RCSB Protein Data Bank. Both bond orders and hydrogen atoms were assigned, and water molecules were removed. The size of box was set to 14Å×14Å×14Å centered in native ligand. Both the native ligand and compound **5** were built using 2D Sketcher and were prepared with LigPrep at OPLS force field, which were docked into the well-defined docking grids with the extra precision (XP) mode. Figure 6 were generated with PyMOL version 1.3.

Acknowledgements

This work was supported by the China National Key Hi-Tech Innovation Project for the R&D of Novel Drugs (No.2013ZX09301303-002).

Conflict of interest

The authors declare no conflict of interest.

Abbreviations

ABC Activated B cell-like; BCR B-cell receptor; BTK Bruton's tyrosine kinase;

DAST Diethylaminosulphur trifluoride; DIBALH Diisobutyl aluminium hydride;

DIPEA *N,N*-Diisopropylethylamine; DLBCL Diffuse large B-cell lymphoma;

EDCI 1-(3-Dimethylaminopropyl)-3-ethylcarbodiimide hydrochloride;

GCB Germinal center B-cell-like;

HATU Hexafluorophosphate azabenzotriazole tetramethyl uronium;

HOBT 1-Hydroxybenzotriazole; IBX 2-Iodoxybenzoic acid;

IKK β Inhibitor of nuclear factor kappa-B kinase;

IRAK4 Interleukin-1 receptor associated kinase 4;
 MYD88 Myeloid differentiation primary response gene 88;
 PDAC Pancreatic ductal adenocarcinoma;
 THP Tetrahydropyranyl.

Reference

- [1] R. Siegel, D. Naishadham, A. Jemal, Cancer statistics, 2013, *CA-Cancer J. Clin.* 63 (2013) 11-30.
- [2] A.A. Alizadeh, M.B. Eisen, R.E. Davis, C. Ma, I.S. Lossos, A. Rosenwald, J.G. Boldrick, H. Sabet, T. Tran, X. Yu, J.I. Powell, L.M. Yang, G.E. Marti, T. Moore, J. Hudson, L.S. Lu, D.B. Lewis, R. Tibshirani, G. Sherlock, W.C. Chan, T.C. Greiner, D.D. Weisenburger, J.O. Armitage, R. Warnke, R. Levy, W. Wilson, M.R. Grever, J.C. Byrd, D. Botstein, P.O. Brown, L.M. Staudt, Distinct types of diffuse large B-cell lymphoma identified by gene expression profiling, *Nature* 403 (2000) 503-511.
- [3] Y.B. Yang, A.L. Shaffer, N.C.T. Emre, M. Ceribelli, M.L. Zhang, G. Wright, W.M. Xiao, J. Powell, J. Platig, H. Kohlhammer, R.M. Young, H. Zhao, Y.D. Yang, W.H. Xu, J.J. Buggy, S. Balasubramanian, L.A. Mathews, P. Shinn, R. Guha, M. Ferrer, C. Thomas, T.A. Waldmann, L.M. Staudt, Exploiting synthetic lethality for the therapy of ABC diffuse large B cell lymphoma, *Cancer Cell* 21 (2012) 723-737.
- [4] R.E. Davis, V.N. Ngo, G. Lenz, P. Tolar, R.M. Young, P.B. Romesser, H. Kohlhammer, L. Lamy, H. Zhao, Y.D. Yang, W.H. Xu, A.L. Shaffer, G. Wright, W.M. Xiao, J. Powell, J.K. Jiang, C.J. Thomas, A. Rosenwald, G. Ott, H.K. Muller-Hermelink, R.D. Gascoyne, J.M. Connors, N.A. Johnson, L.M. Rimsza, E. Campo, E.S. Jaffe, W.H. Wilson, J. Delabie, E.B. Smeland, R.I. Fisher, R.M. Braziel, R.R. Tubbs, J.R. Cook, D.D. Weisenburger, W.C. Chan, S.K. Pierce, L.M. Staudt, Chronic active B-cell-receptor signalling in diffuse large B-cell lymphoma, *Nature* 463 (2010) 88-U97.
- [5] W.H. Wilson, R.M. Young, R. Schmitz, Y. Yang, S. Pittaluga, G. Wright, C.J. Lih, P.M. Williams, A.L. Shaffer, J. Gerecitano, S. de Vos, A. Goy, V.P. Kenkre, P.M. Barr, K.A. Blum, A. Shustov, R. Advani, N.H. Fowler, J.M. Vose, R.L. Elstrom, T.M. Habermann, J.C. Barrientos, J. McGreivy, M. Fardis, B.Y. Chang, F. Clow, B. Munneke, D. Moussa, D.M. Beaupre, L.M. Staudt, Targeting B cell receptor signaling with ibrutinib in diffuse large B cell lymphoma, *Nat. Med.* 21 (2015) 922-926.
- [6] V.N. Ngo, R.M. Young, R. Schmitz, S. Jhavar, W. Xiao, K.-H. Lim, H. Kohlhammer, W. Xu, Y. Yang, H. Zhao, A.L. Shaffer, P. Romesser, G. Wright, J. Powell, A. Rosenwald, H.K. Muller-Hermelink, G. Ott, R.D. Gascoyne, J.M. Connors, L.M. Rimsza, E. Campo, E.S. Jaffe, J. Delabie, E.B. Smeland, R.I. Fisher, R.M. Braziel, R.R. Tubbs, J.R. Cook, D.D. Weisenburger, W.C. Chan, L.M. Staudt, Oncogenically active MYD88 mutations in human lymphoma, *Nature* 470 (2010) 115-119.
- [7] S. Vollmer, S. Strickson, T. Zhang, N. Gray, K.L. Lee, V.R. Rao, P. Cohen, The mechanism of activation of IRAK1 and IRAK4 by interleukin-1 and Toll-like receptor agonists, *Biochem J.* 474 (2017) 2027-2038.
- [8] S.C. Lin, Y.C. Lo, H. Wu, Helical assembly in the MyD88-IRAK4-IRAK2 complex in TLR/IL-1R signalling, *Nature* 465 (2010) 885-U882.
- [9] C.C. Coombs, M.S. Tallman, R.L. Levine, Molecular therapy for acute myeloid leukaemia, *Nat. Rev. Clin. Oncol.* 13 (2016) 305-318.
- [10] S.Y. Li, A. Strelow, E.J. Fontana, H. Wesche, IRAK-4: A novel member of the IRAK family with the properties of an IRAK-kinase, *Proc. Natl. Acad. Sci. U. S. A.* 99 (2002) 5567-5572.
- [11] D. Zhang, L. Li, H. Jiang, Q. Li, A. Wang-Gillam, J. Yu, R. Head, J. Liu, M.B. Ruzinova, K.H. Lim,

Tumor-stroma IL1beta-IRAK4 feedforward circuitry drives tumor fibrosis, chemoresistance, and poor prognosis in pancreatic cancer, *Cancer Res.* 78 (2018) 1700-1712.

[12] D. Zhang, L. Li, H. Jiang, B.L. Knolhoff, A.C. Lockhart, A. Wang-Gillam, D.G. DeNardo, M.B. Ruzinova, K.H. Lim, Constitutive IRAK4 activation underlies poor prognosis and chemoresistance in pancreatic ductal adenocarcinoma, *Clin. Cancer Res.* 23 (2017) 1748-1759.

[13] C.L. Ku, H. von Bernuth, C. Picard, S.Y. Zhang, H.H. Chang, K. Yang, M. Chrabieh, A.C. Issekutz, C.K. Cunningham, J. Gallin, S.M. Holland, C. Roifman, S. Ehl, J. Smart, M. Tang, F.J. Barrat, O. Levy, D. McDonald, N.K. Day-Good, R. Miller, H. Takada, T. Hara, S. Al-Hajjar, A. Al-Ghonaïum, D. Speert, D. Sanlaville, X. Li, F. Geissmann, E. Vivier, L. Marodi, B.Z. Garty, H. Chapel, C. Rodriguez-Gallego, X. Bossuyt, L. Abel, A. Puel, J.L. Casanova, Selective predisposition to bacterial infections in IRAK-4-deficient children: IRAK-4-dependent TLRs are otherwise redundant in protective immunity, *J. Exp. Med.* 204 (2007) 2407-2422.

[14] H. von Bernuth, C. Picard, Z. Jin, R. Pankla, H. Xiao, C.L. Ku, M. Chrabieh, I.B. Mustapha, P. Ghandil, Y. Camcioglu, J. Vasconcelos, N. Sirvent, M. Guedes, A.B. Vitor, M.J. Herrero-Mata, J.I. Arostegui, C. Rodrigo, L. Alsina, E. Ruiz-Ortiz, M. Juan, C. Fortuny, J. Yague, J. Anton, M. Pascal, H.H. Chang, L. Janniere, Y. Rose, B.Z. Garty, H. Chapel, A. Issekutz, L. Marodi, C. Rodriguez-Gallego, J. Banchereau, L. Abel, X. Li, D. Chaussabel, A. Puel, J.L. Casanova, Pyogenic bacterial infections in humans with MyD88 deficiency, *Science* 321 (2008) 691-696.

[15] W.T. McElroy, Interleukin-1 receptor-associated kinase 4 (IRAK4) inhibitors: an updated patent review (2016-2018), *Expert Opin. Ther. Patents* 29 (2019) 243-259.

[16] X. Yuan, H. Wu, H. Bu, J. Zhou, H. Zhang, Targeting the immunity protein kinases for immunoncology, *Eur. J. Med. Chem.* 163 (2019) 413-427.

[17] K.L. Lee, C.M. Ambler, D.R. Anderson, B.P. Boscoe, A.G. Bree, J.I. Brodfuehrer, J.S. Chang, C. Choi, S. Chung, K.J. Curran, J.E. Day, C.M. Dehnhardt, K. Dower, S.E. Drozda, R.K. Frisbie, L.K. Gavrin, J.A. Goldberg, S. Han, M. Hegen, D. Hepworth, H.R. Hope, S. Kamtekar, I.C. Kilty, A. Lee, L.L. Lin, F.E. Lovering, M.D. Lowe, J.P. Mathias, H.M. Morgan, E.A. Murphy, N. Papaioannou, A. Patny, B.S. Pierce, V.R. Rao, E. Saiah, I.J. Samardjiev, B.M. Samas, M.W.H. Shen, J.H. Shin, H.H. Soutter, J.W. Strohbach, P.T. Symanowicz, J.R. Thomason, J.D. Trzuppek, R. Vargas, F. Vincent, J. Yan, C.W. Zapf, S.W. Wright, Discovery of clinical candidate 1-[[2S,3S,4S]-3-ethyl-4-fluoro-5-oxopyrrolidin-2-yl]methoxy]-7-methoxyisoquinoline-6-carboxamide (PF-06650833), a potent, selective Inhibitor of Interleukin-1 Receptor Associated Kinase 4 (IRAK4), by fragment-based drug design, *J. Med. Chem.* 60 (2017) 5521-5542.

[18] V.R. Gummadi, S. Samajdar, Bicyclic heterocycl derivatives as IRAK4 inhibitors, WO2015104688, July 16, 2015.

[19] R.S. Bhide, A. Keon, C. Weigelt, J.S. Sack, R.J. Schmidt, S. Lin, H.Y. Xiao, S.H. Spergel, J. Kempson, W.J. Pitts, J. Carman, M.A. Poss, Discovery and structure-based design of 4,6-diaminonicotinamides as potent and selective IRAK4 inhibitors, *Bioorg. Med. Chem. Lett.* 27 (2017) 4908-4913.

[20] S. Dudhgaonkar, S. Ranade, J. Nagar, S. Subramani, D.S. Prasad, P. Karunanithi, R. Srivastava, K. Venkatesh, S. Selvam, P. Krishnamurthy, T.T. Mariappan, A. Saxena, L. Fan, D.K. Stetsko, D.A. Holloway, X. Li, J. Zhu, W.P. Yang, S. Ruepp, S. Nair, J. Santella, J. Duncia, J. Hynes, K.W. McIntyre, J.A. Carman, Selective IRAK4 inhibition attenuates disease in murine lupus models and demonstrates steroid sparing activity, *J. Immunol.* 198 (2017) 1308-1319.

[21] P.N. Kelly, D.L. Romero, Y. Yang, A.L. Shaffer III, D. Chaudhary, S. Robinson, W. Miao, L. Rui, W.F. Westlin, R. Kapeller, L.M. Staudt, Selective interleukin-1 receptor-associated kinase 4 inhibitors for the

- treatment of autoimmune disorders and lymphoid malignancy, *J. Exp. Med.* 212 (2015) 2189-2201.
- [22] S.L. Degorce, R. Anjum, K.S. Dillman, L. Drew, S.D. Groombridge, C.T. Halsall, E.M. Lenz, N.A. Lindsay, M.F. Mayo, J.H. Pink, G.R. Robb, J.S. Scott, S. Stokes, Y. Xue, Optimization of permeability in a series of pyrrolotriazine inhibitors of IRAK4, *Bioorg. Med. Chem.* 26 (2018) 913-924.
- [23] J.S. Scott, S.L. Degorce, R. Anjum, J. Culshaw, R.D.M. Davies, N.L. Davies, K.S. Dillman, J.E. Dowling, L. Drew, A.D. Ferguson, S.D. Groombridge, C.T. Halsall, J.A. Hudson, S. Lamont, N.A. Lindsay, S.K. Marden, M.F. Mayo, J.E. Pease, D.R. Perkins, J.H. Pink, G.R. Robb, A. Rosen, M. Shen, C. McWhirter, D. Wu, Discovery and optimization of pyrrolopyrimidine inhibitors of interleukin-1 receptor associated kinase 4 (IRAK4) for the treatment of mutant MYD88(L265P) diffuse large B-cell lymphoma, *J. Med. Chem.* 60 (2017) 10071-10091.
- [24] M.C. Bryan, J. Drobnick, A. Gobbi, A. Kolesnikov, Y. Chen, N. Rajapaksa, C. Ndubaku, J. Feng, W. Chang, R. Francis, C. Yu, E.F. Choo, K. DeMent, Y. Ran, L. An, C. Emson, Z. Huang, S. Sujatha-Bhaskar, H. Brightbill, A. DiPasquale, J. Maher, J. Wai, B.S. McKenzie, P.J. Lupardus, A.A. Zarrin, J.R. Kiefer, Development of potent and selective pyrazolopyrimidine IRAK4 inhibitors, *J. Med. Chem.* 62 (2019) 6223-6240.
- [25] J. Lim, M.D. Altman, J. Baker, J.D. Brubaker, H. Chen, Y. Chen, T. Fischmann, C. Gibeau, M.A. Kleinschek, E. Leccese, C. Lesburg, J.K. Maclean, L.Y. Moy, E.F. Mulrooney, J. Presland, L. Rakhilina, G.F. Smith, D. Steinhuebel, R. Yang, Discovery of 5-amino-*N*-(1*H*-pyrazol-4-yl)pyrazolo[1,5-*a*]pyrimidine-3-carboxamide inhibitors of IRAK4, *ACS Med. Chem. Lett.* 6 (2015) 683-688.
- [26] W.T. McElroy, Z. Tan, G. Ho, S. Paliwal, G. Li, W.M. Seganish, D. Tulshian, J. Tata, T.O. Fischmann, C. Sondey, H. Bian, L. Bober, J. Jackson, C.G. Garlisi, K. Devito, J. Fossetta, D. Lundell, X. Niu, Potent and selective amidopyrazole inhibitors of IRAK4 that are efficacious in a rodent model of inflammation, *ACS Med. Chem. Lett.* 6 (2015) 677-682.
- [27] S. Cherukupalli, R. Karpoornath, B. Chandrasekaran, G.A. Hampannavar, N. Thapliyal, V.N. Palakollu, An insight on synthetic and medicinal aspects of pyrazolo[1,5-*a*]pyrimidine scaffold, *Eur. J. Med. Chem.* 126 (2017) 298-352.
- [28] T. Paino, A. Garcia-Gomez, L. Gonzalez-Mendez, L. San-Segundo, S. Hernandez-Garcia, A.A. Lopez-Iglesias, E.M. Algarin, M. Martin-Sanchez, D. Corbacho, C. Ortiz-de-Solorzano, L.A. Corchete, N.C. Gutierrez, M.V. Maetos, M. Garayoa, E.M. Ocio, The novel pan-PIM kinase inhibitor, PIM447, displays dual antimyeloma and bone-protective effects, and potently synergizes with current standards of care, *Clin. Cancer Res.* 23 (2017) 225-238.
- [29] T. Peng, J.R. Wu, L.J. Tong, M.Y. Li, F. Chen, Y.X. Leng, R. Qu, K. Han, Y. Su, Y. Chen, W.H. Duan, H. Xie, J. Ding, Identification of DW532 as a novel anti-tumor agent targeting both kinases and tubulin, *Acta Pharmacol. Sin.* 35 (2014) 916-928.

Highlights

1. A series of imidazo[1,2-*b*]pyridazine derivatives were designed and synthesized.
2. Compound **5** displayed excellent IRAK4 potency (IRAK4 IC₅₀ = 1.3 nM) and favorable kinase selectivity profile.
3. Compound **5** selectively reduced the viability of mMYD88 cell lines, OCI-LY10 and TMD8.
4. Compound **5** effectively inhibited the activation of IRAK4-IKK β -NF- κ B signaling.
5. Compound **5** and ibrutinib synergistically exhibited anti-tumor activity to TMD8 cells.

Declaration of interests

The authors declare that they have no known competing financial interests or personal relationships that could have appeared to influence the work reported in this paper.

The authors declare the following financial interests/personal relationships which may be considered as potential competing interests:

Journal Pre-proof